Precision Electroweak Measurements in ATLAS and CMS

Daniele Zanzi
on behalf of ATLAS and CMS collaborations

LHCP 2019, Puebla, Mexico

Outline

$$\sin^2\theta_W = 1 - M_W^2/M_Z^2$$

- W mass measurement
- $\sin^2\theta_W$ measurement
- Recent W,Z cross section measurements:
  - Z $d\sigma/dm$ at 13TeV
  - Z $d\sigma/p_T$, $d\sigma/d\phi^*$, $d\sigma/dy$ at 13TeV
  - W production and charge asymmetry at 8TeV
  - W,Z at 5.02 TeV
- Related talks:
  - Electroweak precision measurements with ATLAS (Elena Yatsenko) and CMS (Dylan George Hsu)

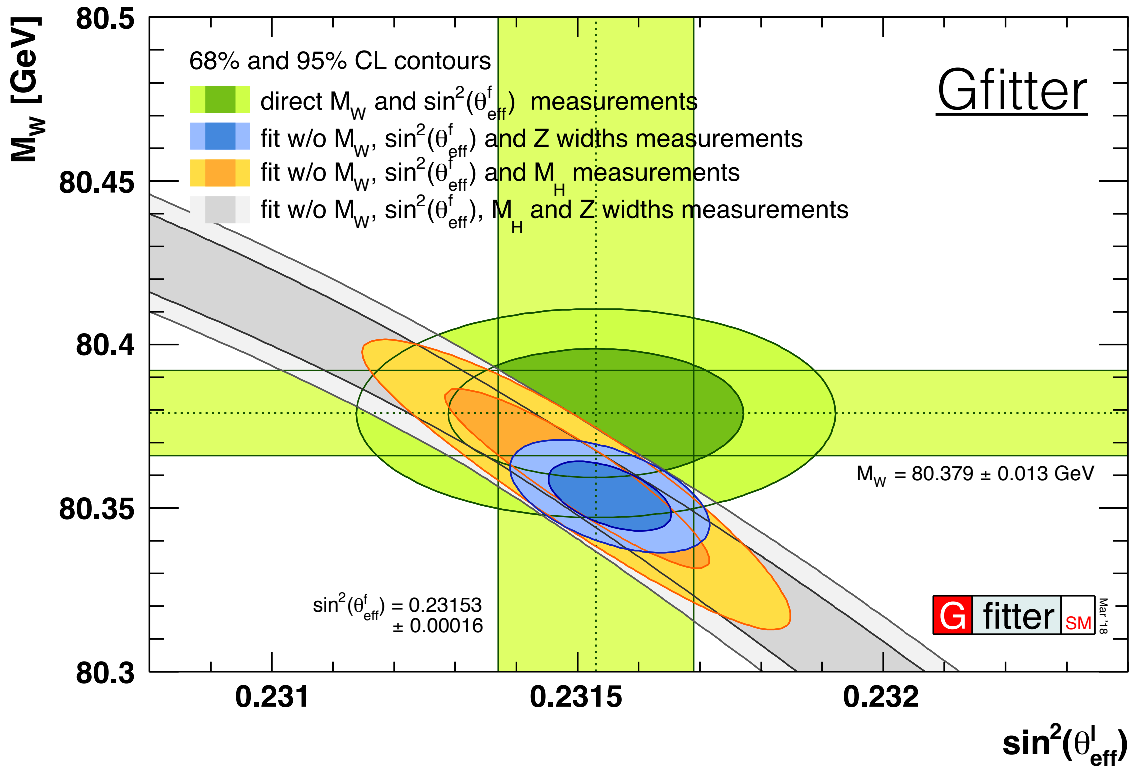

Introduction

- $\sin^2\theta_W$ and m_W are key parameters of the SM
  - can be calculated from m_Z, α_{EM}, G_μ (with corrections from m_{top} and m_H)
- To test SM, our goal is to reach the precision of global EW fit with direct measurements:
  - m_W at ±10MeV
  - $\sin^2\theta_W$ at ≲±10^{-4}
- LHC individual experiments approaching sensitivity of LEP/SLD and Tevatron combined
  - But PDF uncertainties are becoming the bottleneck

$$\sin^2\theta_W = 1 - M_W^2/M_Z^2$$

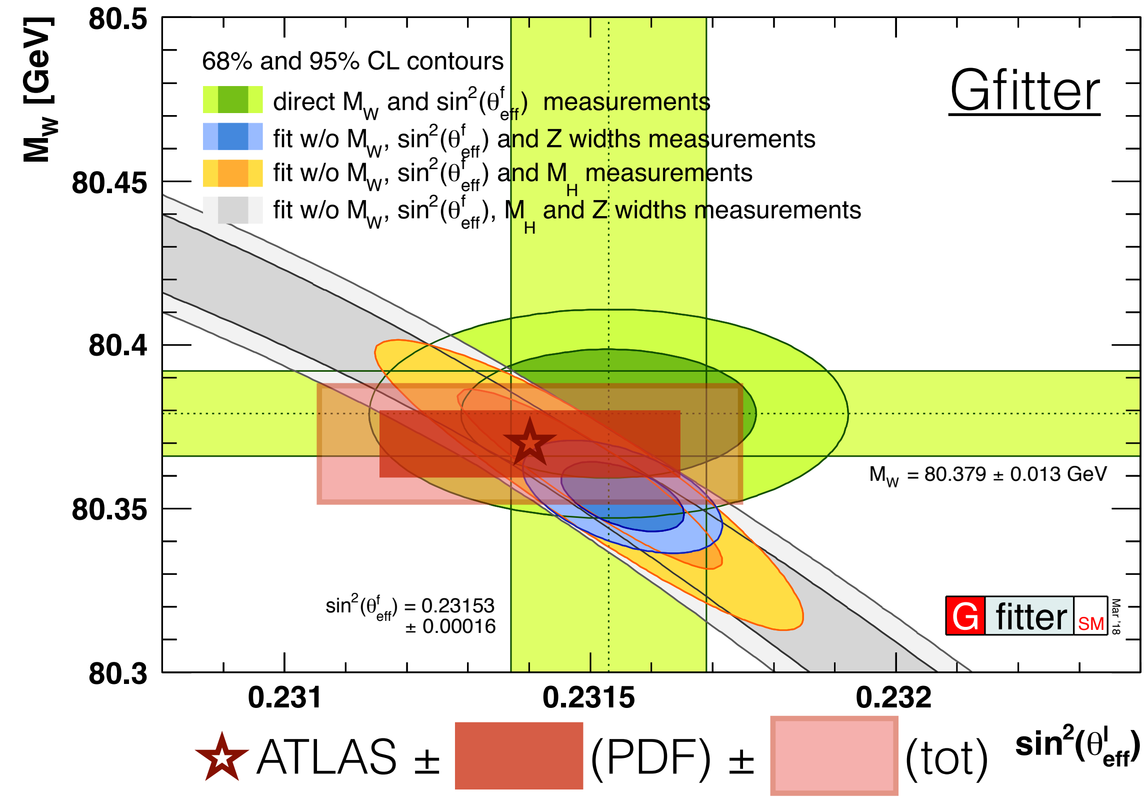

	EW Fit	World Avg
sin2θW	0.23153 ± 0.0000**6**	0.23152 ± 0.000**16**
mW [GeV]	80.354 ± 0.00**7**	80.379 ± 0.0**13**

gFitter

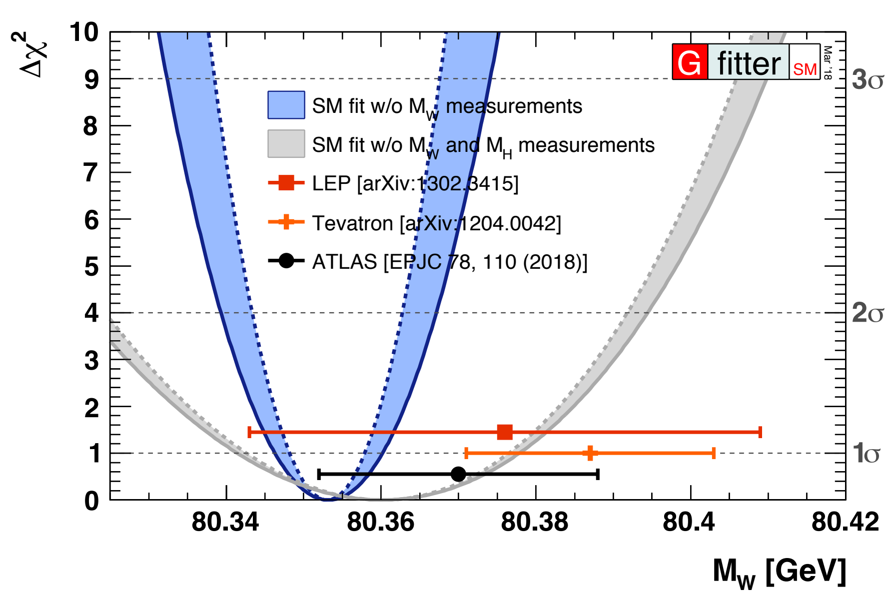

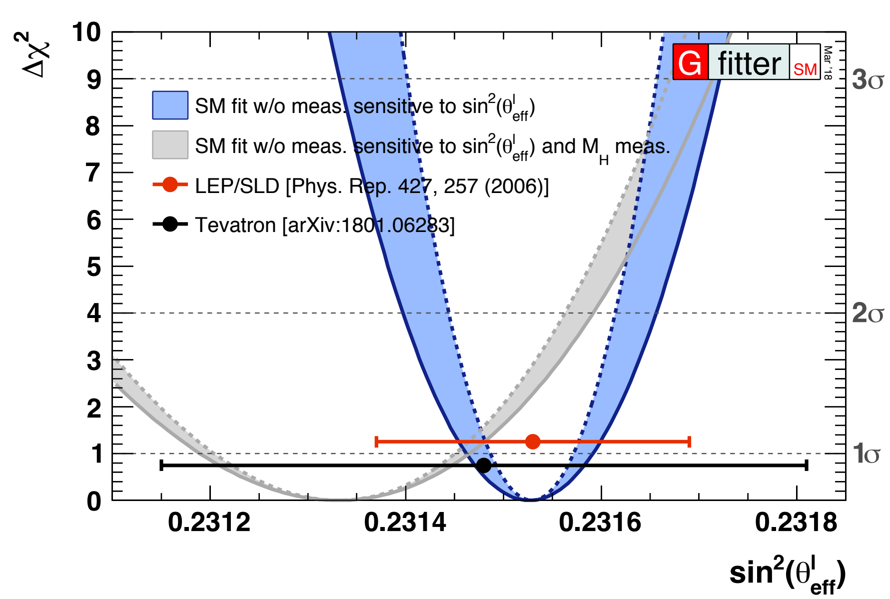

D. Zanzi

W Mass

W Mass

EPJC78(2018)110

- Measured with 4.6 fb^{-1} at 7 TeV by ATLAS
  - both $W \rightarrow e\nu$ and $W \rightarrow \mu\nu$ channels analysed
- Template fit to p_T^l and m_T
  - p_T^l sensitive to p_T^W modelling
  - m_T sensitive to hadronic recoil u_T
- Templates built with Powheg+Pythia8 and reweighted to best theoretical modelling
  - $d\sigma/d\eta$ and W polarisation with DYNNLO
  - $d\sigma/dpT$ with Pythia8 and AZ tune

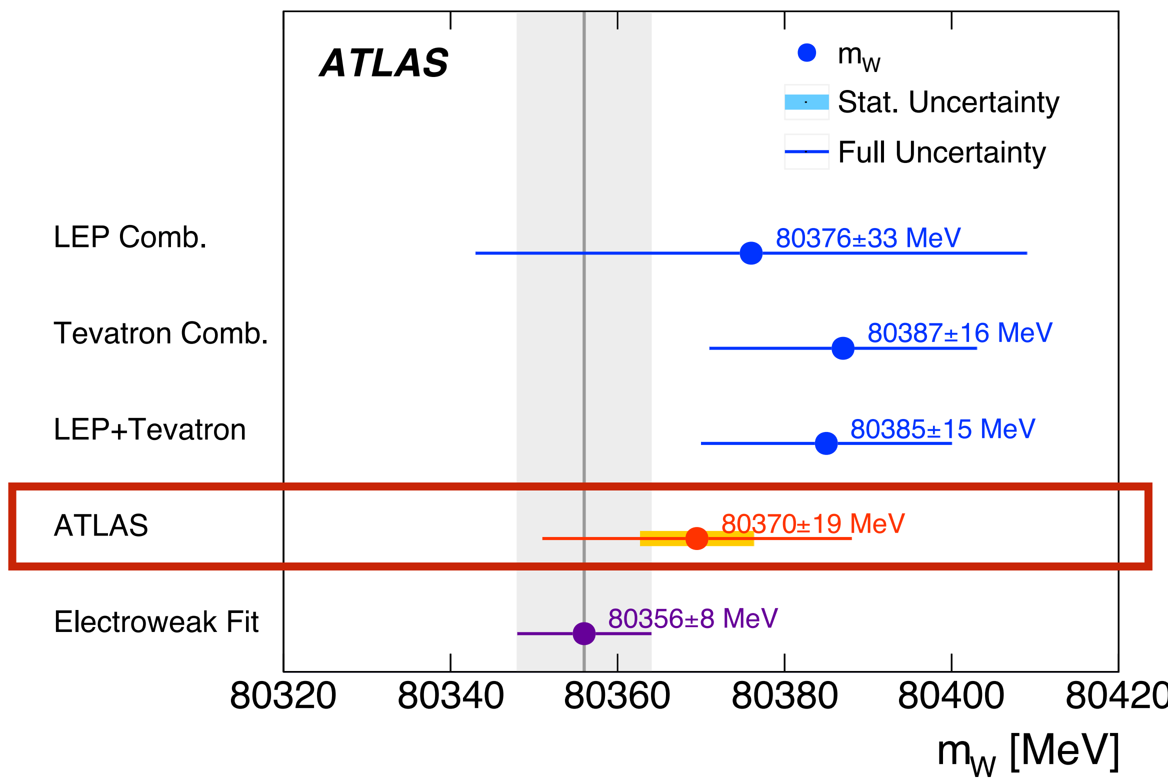

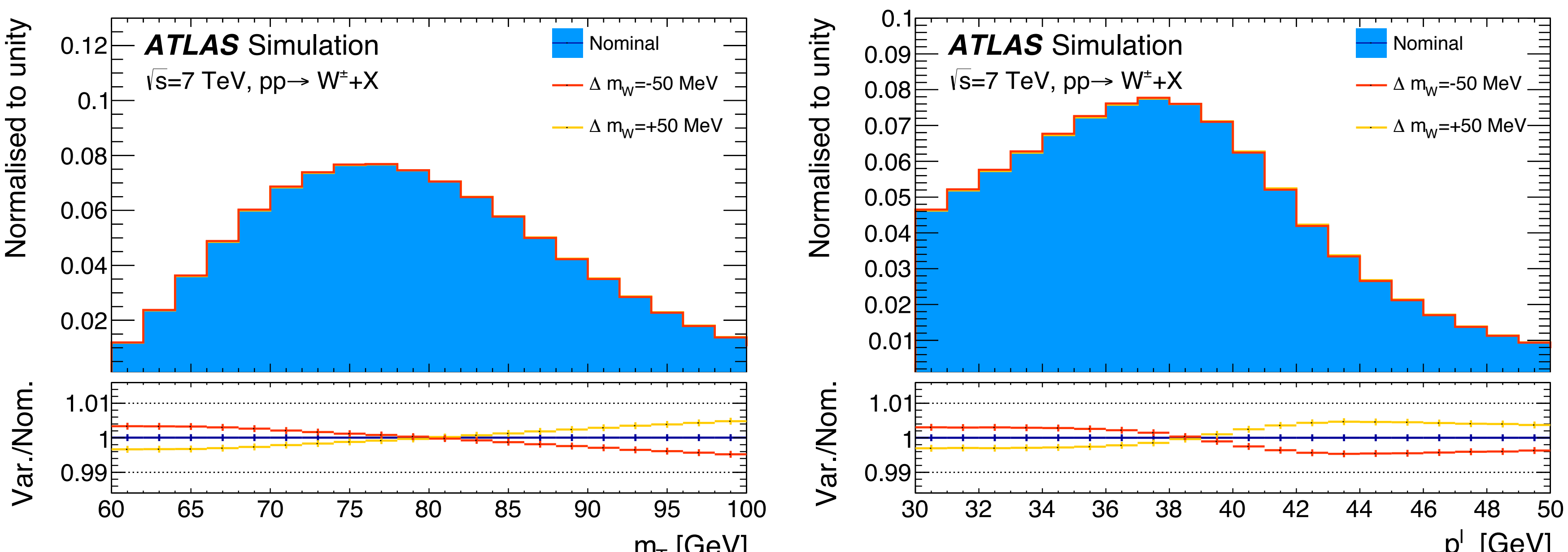

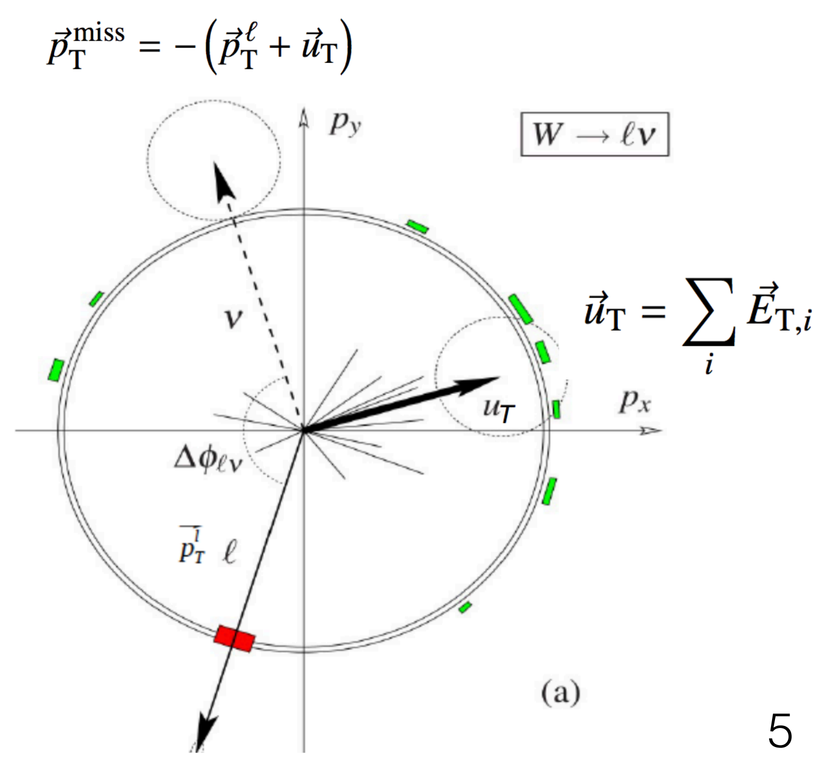

m_W Uncertainties

ATL-PHYS-PUB-2017-021

Combined categories	Value [MeV]	Stat. Unc.	Muon Unc.	Elec. Unc.	Recoil Unc.	Bckg. Unc.	QCD Unc.	EW Unc.	PDF Unc.	Total Unc.	χ^2/dof of Comb.
m_T-p_T^ℓ, $W^\pm$, e-μ	80369.5	6.8	6.6	6.4	2.9	4.5	8.3	5.5	9.2	18.5	29/27

- PDF uncertainties
  - lepton distributions affected by W polarisation (sensitive to PDF)
  - p_T^W spectrum dependent on the flavour of the incoming quarks
  - needs for future results:
    - improved precision with more W,Z measurements (and N3LL+NNLO predictions? ATL-PHYS-PUB-2018-004)
    - estimate of correlations among PDF sets for combinations with other m_W and $\sin^2\theta_W$ measurements
- QCD systematics mainly due to uncertainties on p_T^W
  - at 7TeV with $<\mu>$~9, p_T^W precision limited by $\sigma(u_T)$~13GeV resolution on hadronic recoil
  - p_T^W modelled from Z p_T data via Pythia8 AZ tune → 2.5% uncertainty at low p_T from extrapolation syst
  - same 2.5% precision also in W/Z ratio in 8TeV data (CMS)

ATL-PHYS-PUB-2017-021

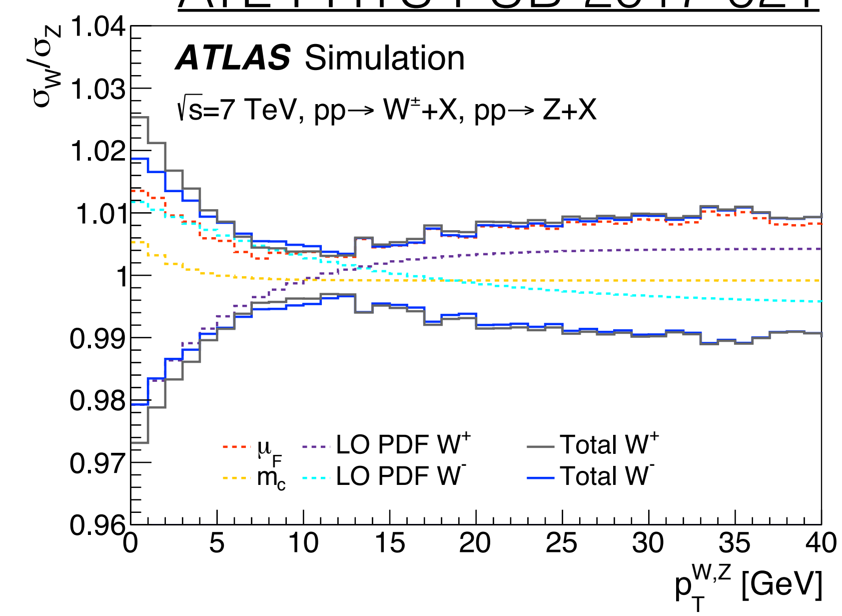

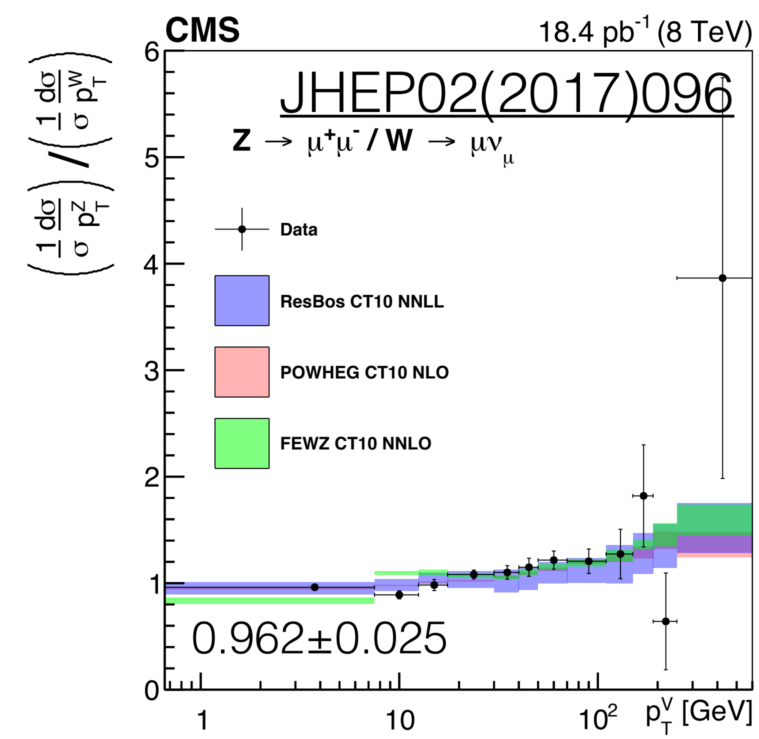

p_T^W Prospects

- Plan to directly measure p_T^W in data in W events at low μ and with good u_T resolution
  - target 1% precision in 5GeV-bins of p_T^W at low p_T → x0.5 QCD modelling syst for W mass
  - requires $\sigma(u_T) \lesssim$5GeV to control bin-by-bin migration syst
  - expected to be achieved with low μ data, lower calorimeter thresholds and new improved particle-flow algorithm for hadronic recoil (EPJC77(2017)466)
- Low-μ datasets, <μ>~2:
  - ATLAS/CMS: 380/200pb^{-1} at 13TeV, 260/300pb^{-1} at 5TeV (preliminary luminosity calibrations)
  - for equal luminosity, 5TeV and 13TeV data expected to have same sensitivity (better u_T resolution at 5TeV, ie lower UE, and higher cross section at 13TeV)

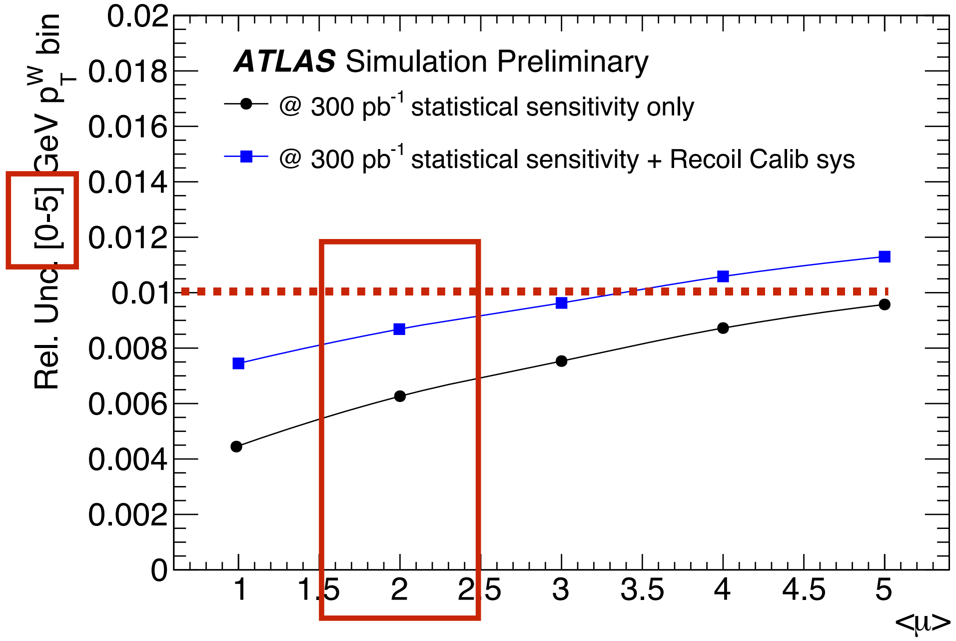

ATL-PHYS-PUB-2017-021

$\sin^2\theta_W$

$\sin^2\theta_W$

- Measured via asymmetry in lepton angular distributions in Z decays induced by the Z coupling structure
- Most-precise measurement from LEP+SLD combination (16×10^{-5}), but with a difference between the two most sensitive individual results at 3.2σ
- At LHC, two related methodologies:
  - A_4 angular coefficients in full decay lepton phase space (ATLAS-CONF-2018-037)
  - triple differential ($\cos\theta_{CS}$, m_{ll}, y_{ll}) cross section and A_{FB} in fiducial phase space (JHEP12(2017)059, EPJC78(2018)701)

ATLAS-CONF-2018-037

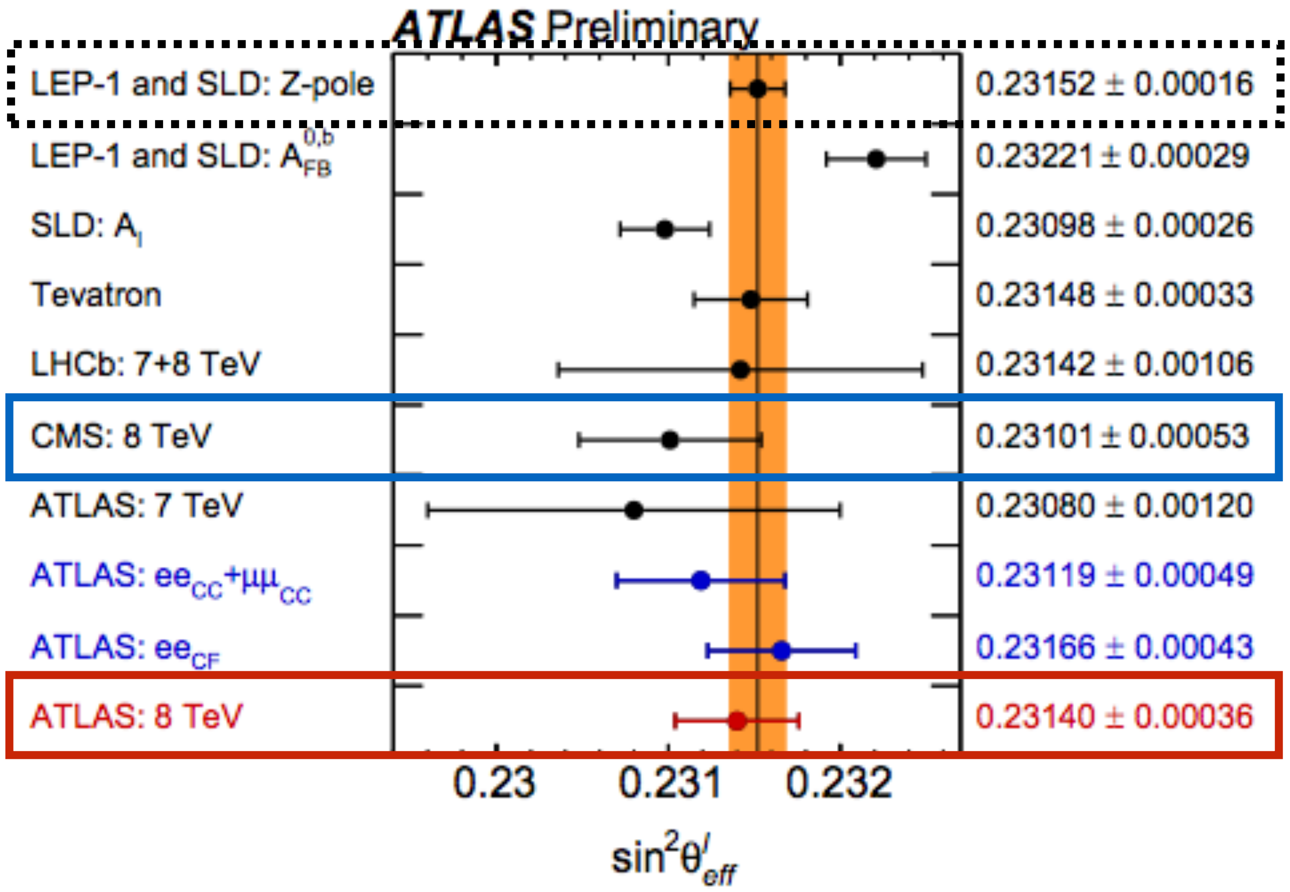

$\sin^2\theta^f_{eff} = \sin^2\theta_W K^f(s,t)$, with K^f fermion-flavour dependent form factors that absorbs EW corrections

Ai Methodology

Collin-Soper frame

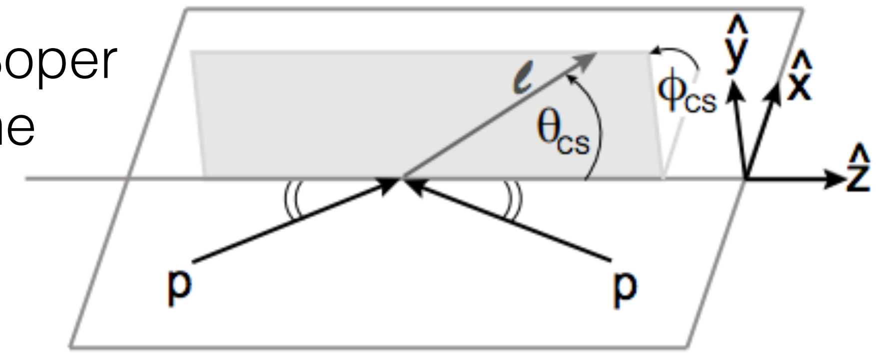

$$\frac{d\sigma}{dp_T^{\ell\ell}\, dy^{\ell\ell}\, dm^{\ell\ell}\, d\cos\theta\, d\phi} = \frac{3}{16\pi} \frac{d\sigma^{U+L}}{dp_T^{\ell\ell}\, dy^{\ell\ell}\, dm^{\ell\ell}} \Big\{ (1+\cos^2\theta) + \frac{1}{2} A_0 (1 - 3\cos^2\theta) + A_1 \sin 2\theta \cos\phi + \frac{1}{2} A_2 \sin^2\theta \cos 2\phi + A_3 \sin\theta \cos\phi + \boxed{A_4 \cos\theta} + A_5 \sin^2\theta \sin 2\phi + A_6 \sin 2\theta \sin\phi + A_7 \sin\theta \sin\phi \Big\}.$$

EW LO and all orders in QCD

- pp→Z→ll cross section in full lepton phase space determined by 5 variables that separate Z production from decay kinematics
  - 9 harmonic polynomials $P_i(\cos\theta_{CS}, \phi_{CS})$ describe the lepton angular distributions in Z rest frame
  - 8 $A_i(m^{ll}, p_T^{ll}, y^{ll})$ coefficients and total unpolarised cross section $\sigma^{U+L}(m^{ll}, p_T^{ll}, y^{ll})$ describe the Z kinematics
- Parity-violating A_4 term sensitive to $\sin^2\theta^f_{eff}$
  - A_4 proportional to $\sin^2\theta^f_{eff}$ based on effective linear relation (including EW corrections)
  - 10^{-4} in A_4 → $2*10^{-5}$ in $\sin^2\theta^f_{eff}$
  - in decay lepton full phase space $A_{FB} = 3/8\, A_4$

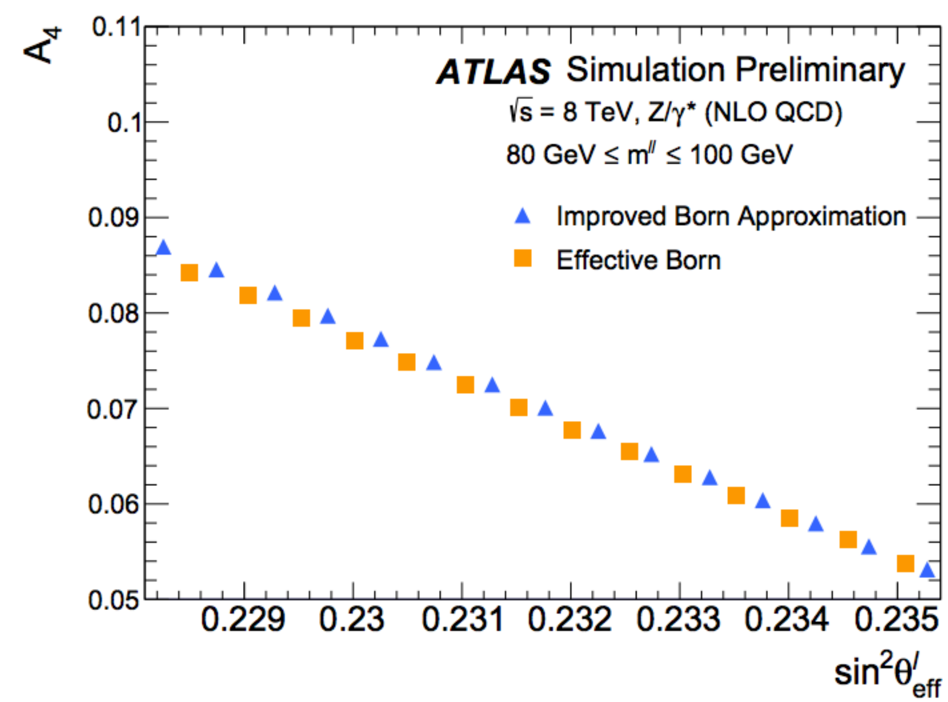

ATLAS-CONF-2018-037

Ai Methodology

Collin-Soper frame

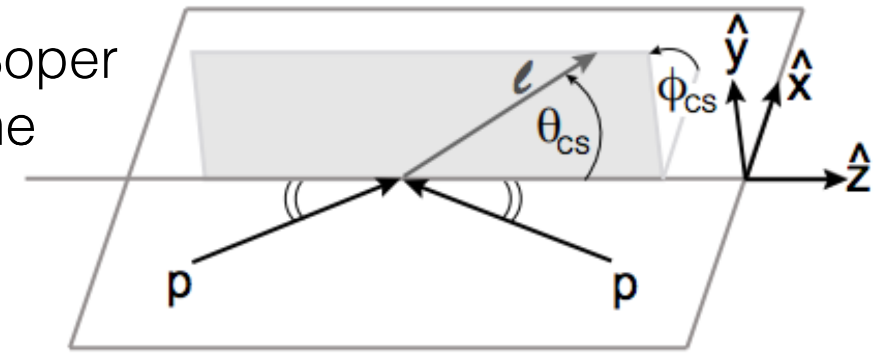

$$\frac{d\sigma}{dp_T^{\ell\ell}\, dy^{\ell\ell}\, dm^{\ell\ell}\, d\cos\theta\, d\phi} = \frac{3}{16\pi} \frac{d\sigma^{U+L}}{dp_T^{\ell\ell}\, dy^{\ell\ell}\, dm^{\ell\ell}} \Big\{(1+\cos^2\theta) + \frac{1}{2} A_0(1-3\cos^2\theta) + A_1 \sin 2\theta \cos\phi + \frac{1}{2} A_2 \sin^2\theta \cos 2\phi + A_3 \sin\theta \cos\phi + A_4 \cos\theta + A_5 \sin^2\theta \sin 2\phi + A_6 \sin 2\theta \sin\phi + A_7 \sin\theta \sin\phi \Big\}.$$

- Fold $P_i(\cos\theta_{CS}, \phi_{CS})$ to detector level
- Fit reconstructed $\cos\theta_{CS}, \phi_{CS}, m_{ll}, y_{ll}$ distributions in born-level m^{ll}, y^{ll} bins
- Extract A_4 in full decay lepton phase space and use predictions of A_4 to infer $\sin^2\theta^f_{eff}$
- A_4 measurement dominated by statistical uncertainties
- QCD and PDF uncertainties dominate $\sin^2\theta^f_{eff}$ interpretation of A_4

fit Ai to data

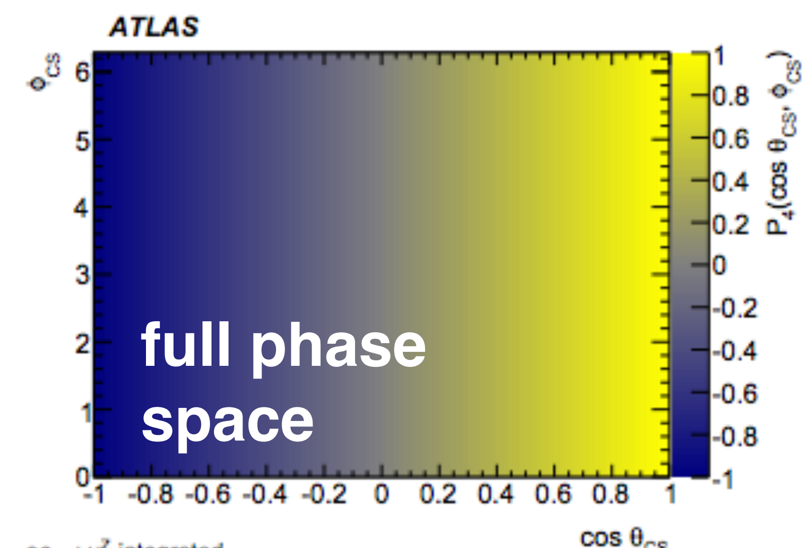

fold detector acceptance

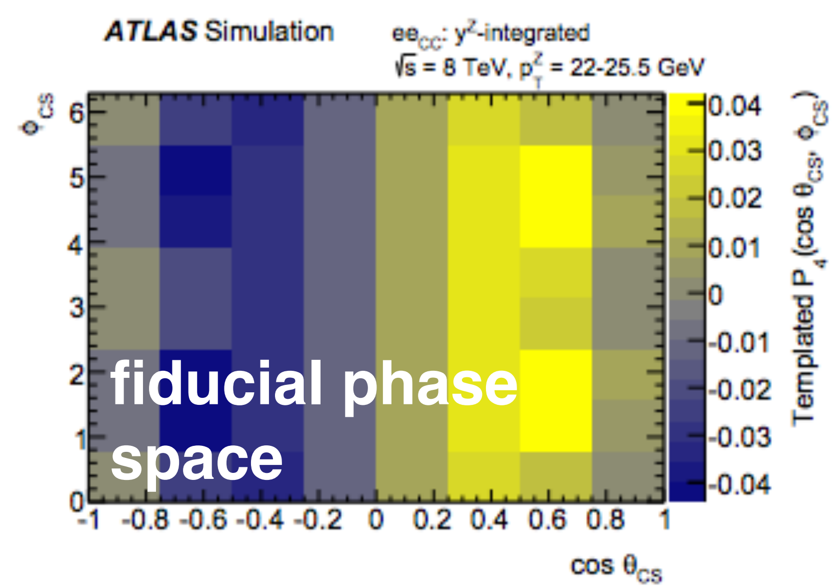

A_{FB} Methodology

- Measure of A_{FB} asymmetry in Collin-Soper frame in reconstructed m_{ll}, y_{ll} bins
  - angular event-weighted A_{FB} to improve statistical uncertainty and reduce impact of efficiency and acceptance uncertainties
- $\sin^2\theta^f_{eff}$ extracted from template fit to A_{FB} in data using predictions (Powheg v2+NNPDF3.0)

$$A_{FB} = \frac{\sigma(\cos\theta^* > 0) - \sigma(\cos\theta^* < 0)}{\sigma(\cos\theta^* > 0) + \sigma(\cos\theta^* < 0)}$$

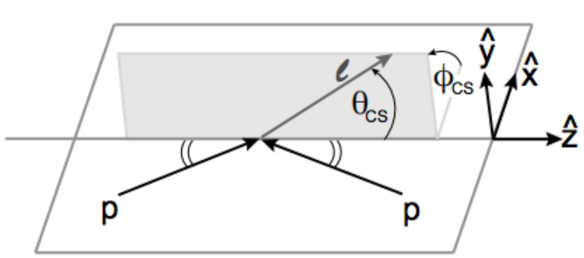

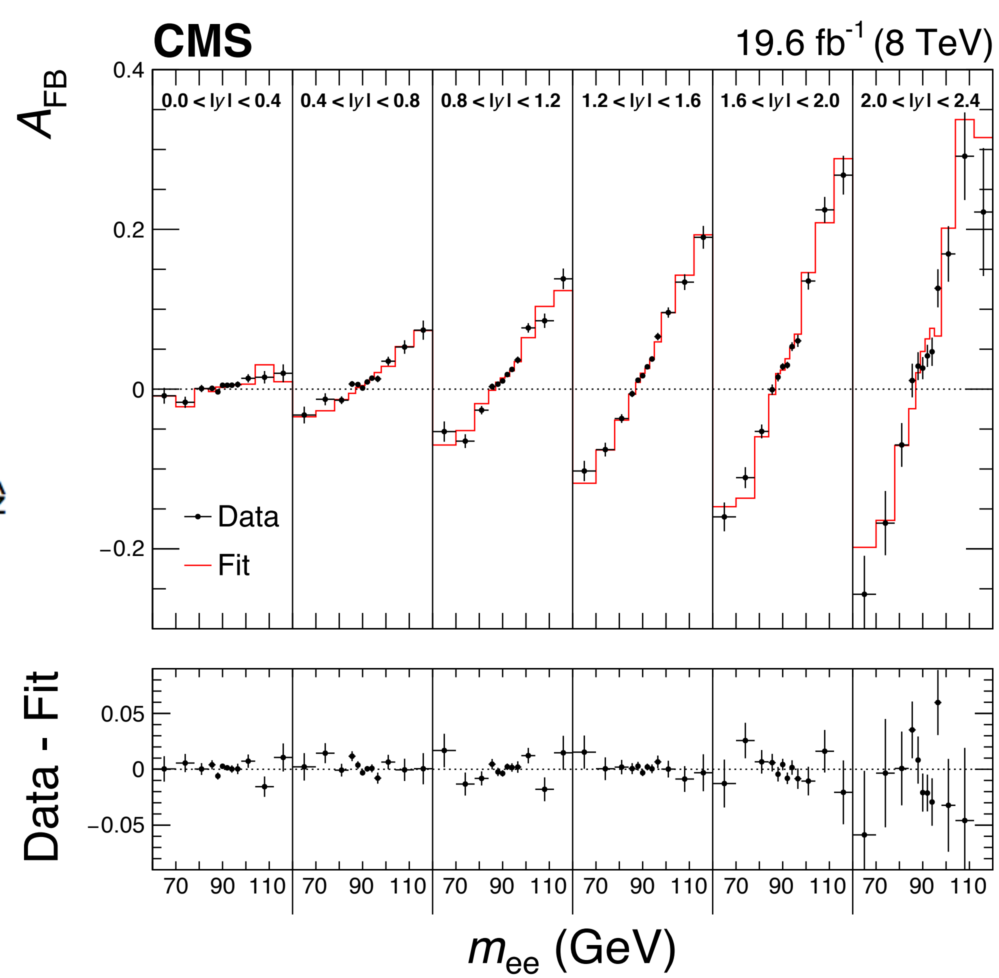

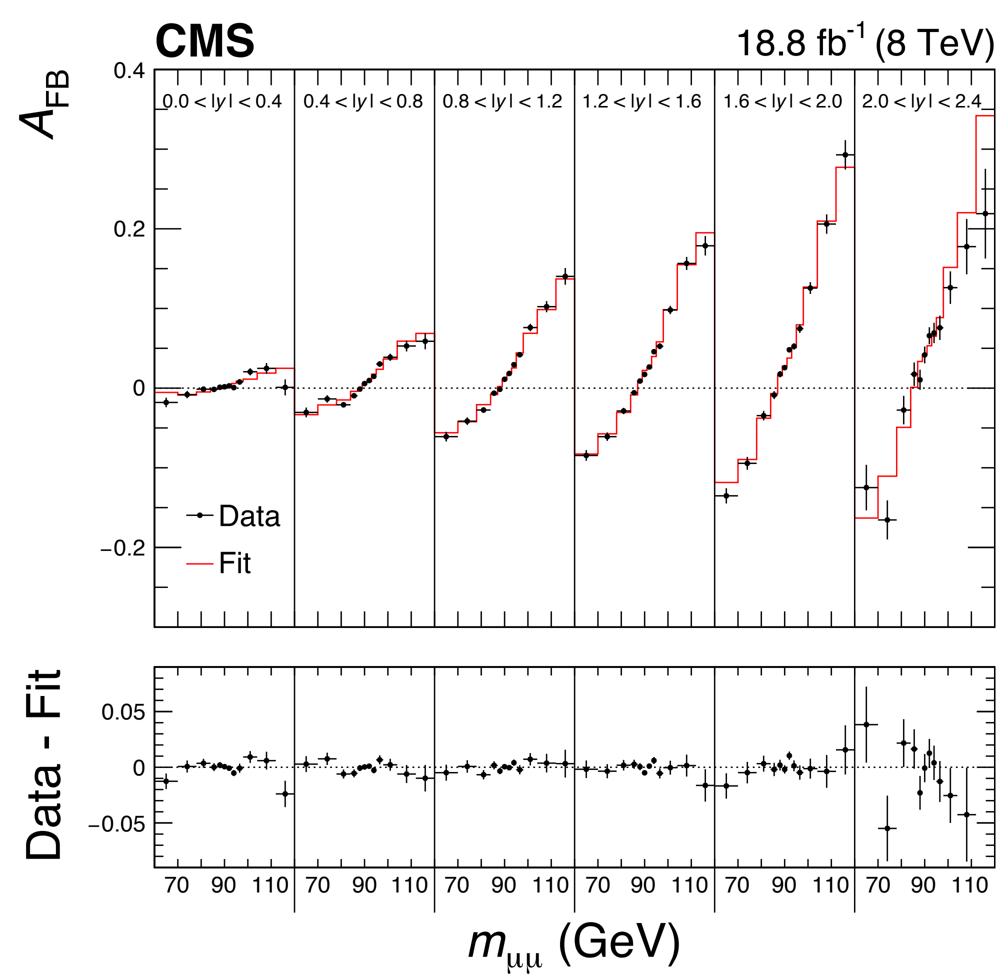

A_{FB},A_4 at LHC

- A_{FB},A_4 strongly depend on PDF
  - quark assigned based on Z rapidity
  - largest at high y^Z where valence quark PDFs dominate at large x
  - also depend on quark flavour, so on relative contributions of u and d PDFs
- $\mu\mu$CC and eeCC channels with central leptons $|\mu|<2.4$ ($|\mu_e|<2.5$ in CMS)
  - high statistics, good to constrain PDFs
  - similar sensitivity in ATLAS and CMS
- eeCF channel with a forward electron $2.5<|\mu|<4.9$
  - low statistics, high sensitivity to $\sin^2\theta^f_{eff}$
  - experimentally challenging, unique to ATLAS

ATL-PHYS-PUB-2018-004

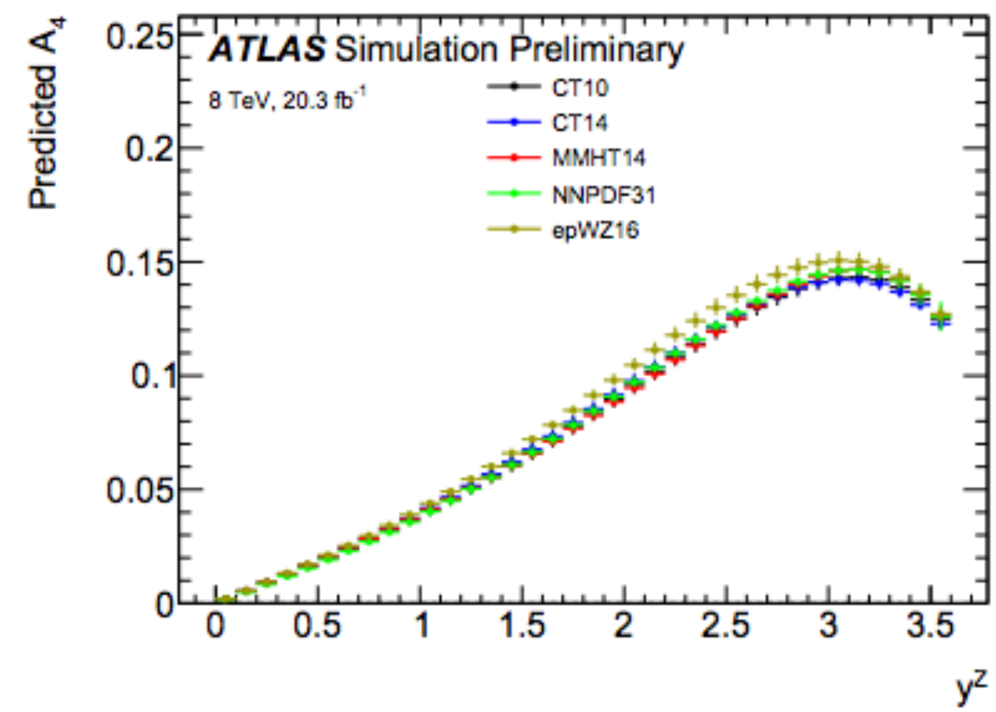

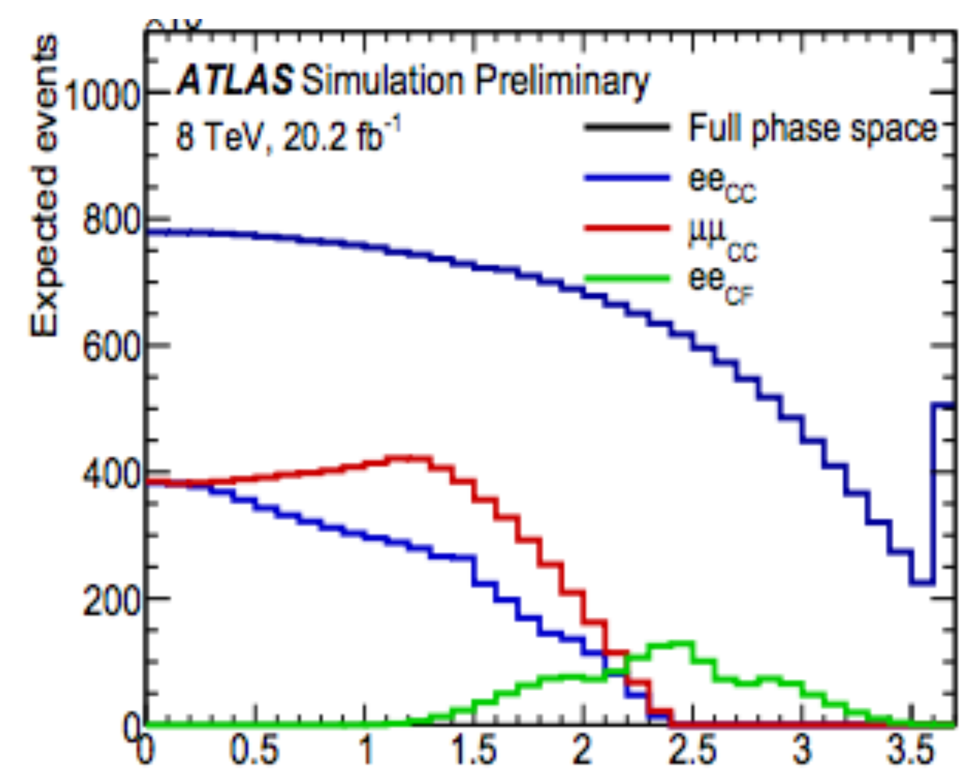

ATLAS-CONF-2018-037

$\sin^2\theta^f_{eff}$

[10^{-5}] **ATLAS** **CMS**

Channel	ee_{CC}	$\mu\mu_{CC}$	ee_{CF}	$ee_{CC}+\mu\mu_{CC}$	$ee_{CC}+\mu\mu_{CC}+ee_{CF}$	CMS eeCC	CMS $\mu\mu$CC	CMS Comb
Central value	0.23148	0.23123	0.23166	0.23119	0.23140			
Uncertainties								
Total	68	59	43	49	36			53
Stat.	48	40	29	31	21	60	44	36
Syst.	48	44	32	38	29			
Uncertainties in measurements								
PDF (meas.)	8	9	7	6	4			
p_T^Z modelling	0	0	7	0	5			
Lepton scale	4	4	4	4	3	19	8	
Lepton resolution	6	1	2	2	1			
Lepton efficiency	11	3	3	2	4	4	5	
Electron charge misidentification	2	0	1	1	< 1			
Muon sagitta bias	0	5	0	1	2			
Background	1	2	1	1	2			
MC. stat.	25	22	18	16	12	33	15	
Uncertainties in predictions								
PDF (predictions)	37	35	22	33	24			31
QCD scales	6	8	9	5	6	14	16	
EW corrections	3	3	3	3	3			

ATLAS-CONF-2018-037   EPJC78(2018)701

$\sin^2\theta^f_{eff}$ and PDFs

- PDF uncertainties constrained in A_{FB},A_4 → $\sin^2\theta^f_{eff}$ interpretation exploiting correlations in m^{ll} and y^{ll}
  - PDF uncertainties profiled in ATLAS
  - Bayesian χ^2 reweighting in CMS
- Yet PDF is source of large systematic uncertainty
  - CMS: PDF syst ±31, spread among PDF sets ~65 [10^{-5}]
  - ATLAS: PDF syst ±24, spread among PDF sets ~28 [10^{-5}]
  - compatibility cannot be estimated without correlations
- Improved understanding of PDF differences and correlations is key
  - new PDF sets with more LHC W,Z data will reduce impact of in-situ PDF constraints and ease combinations

EPJC78(2018)701

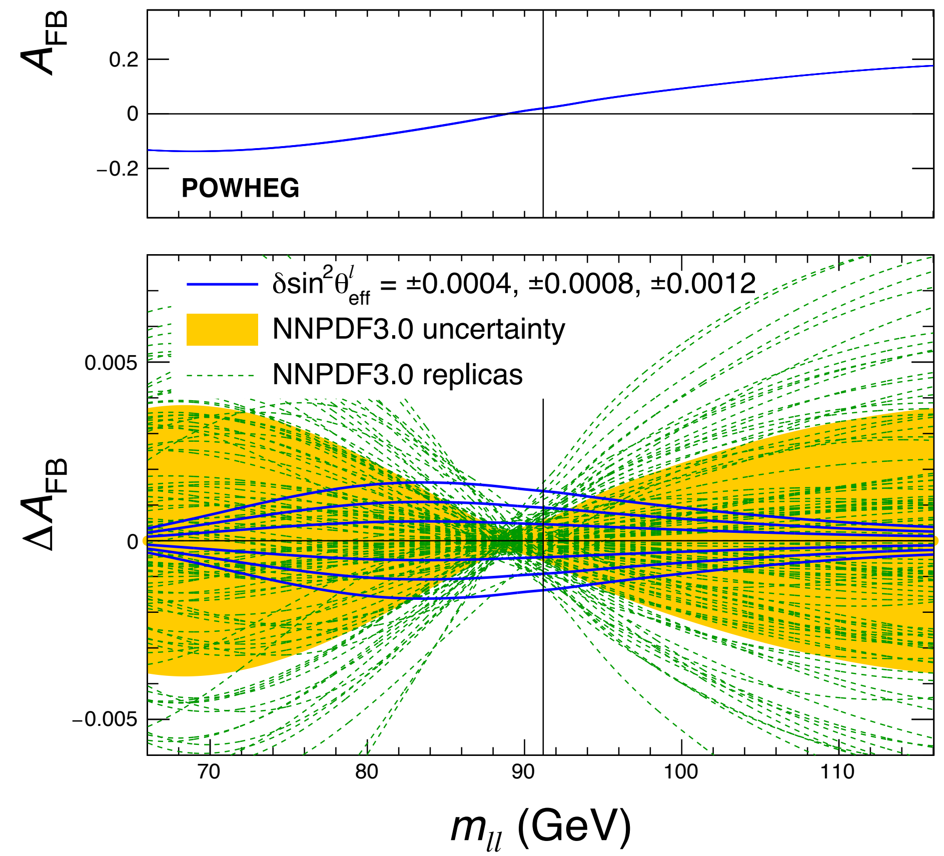

	CT10	CT14	MMHT14	NNPDF31
$\sin^2\theta^\ell_{eff}$	0.23118	0.23141	0.23140	0.23146
	Uncertainties in measurements			
Total	39	37	36	38
Stat.	21	21	21	21
Syst.	32	31	29	31

ATLAS-CONF-2018-037

EPJC78(2018)701

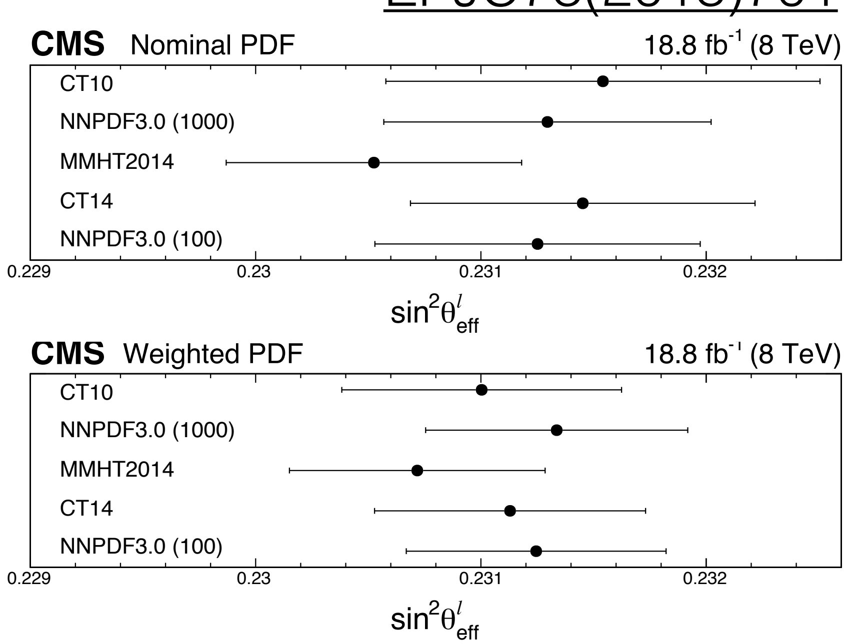

$\sin^2\theta^f_{eff}$ Prospects

- LHC Run1 measurements dominated by statistical and PDF uncertainties
- Future measurements at 13/14TeV:
  - higher statistics can more strongly constrain PDFs
  - higher dilution balanced by higher statistics
- Work ongoing in LHC EW precision group (April meeting in Durham) and PDF4LHC forum to investigate
  - EW/QED corrections, EW schemes, benchmark NNLO and resummed calculations and uncertainties
  - PDF differences and correlations

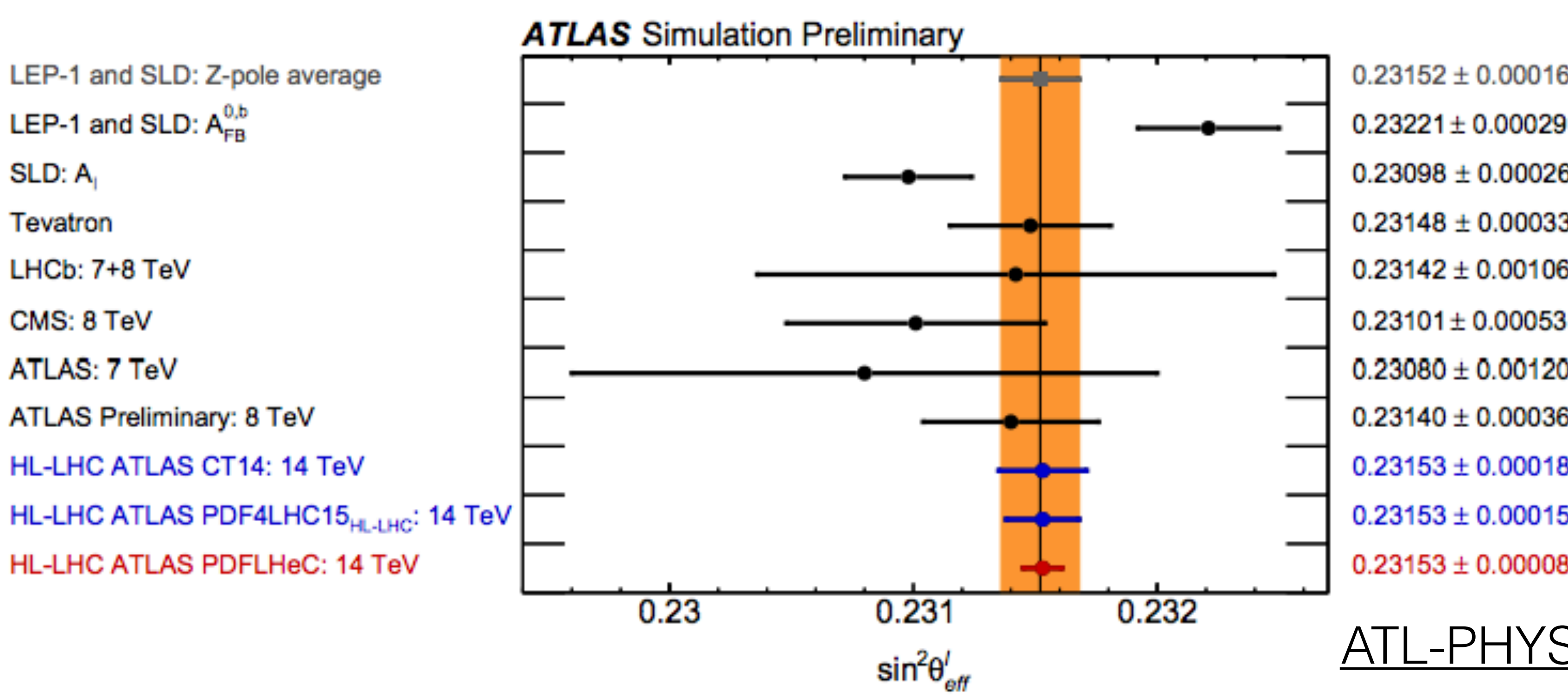

3000fb^{-1}

PDF syst
±24
±16
±13

Recent W,Z Cross Section Measurements

More details in talks by Elena Yatsenko (ATLAS) and Dylan George Hsu (CMS)

W,Z Overview

ATLAS/CMS		2.76 TeV	5 TeV	7 TeV	8 TeV	13 TeV
W	inclusi	STDM-2018-06 (*)				PLB759(2016)6
	dσ/dpt			PRD85(2012)012005	JHEP02(2017)096	
	dσ/dη		**EPJC79(2019) 128**	EPJC77(2017)367	**arXiv:1904.05631 (sub. to EPJC)** EPJC76(2016)469	
	asym		**EPJC79(2019) 128**	EPJC77(2017)367 PRL109(2012)111806 PRD90(2014)032004	**arXiv:1904.05631 (sub. to EPJC)** EPJC76(2016)469	
	mass			EPJC78(2018)110		
Z	inclusi	STDM-2018-06 (*)				PLB759(2016)6
	dσ/dm			PLB725(2013)223 (high-mass), JHEP06(2014)112 (low-mass), EPJC77(2017)367,	JHEP12(2017)059, JHEP08(2016)009 (high mass) EPJC75(2015)147	**arXiv: 1812.10529 (sub. to JHEP)**
	dσ/dpt			JHEP09(2014)145 PRD85(2012)032002	EPJC76(2016)291 JHEP02(2017)096 PLB749(2015)187	**CMS-PAS-SMP-17-010**
	dσ/dη		**EPJC79(2019) 128**	EPJC77(2017)367 PRD85(2012)032002 JHEP12(2013)030	JHEP12(2017)059 EPJC75(2015)147 PLB749(2015)187	**CMS-PAS-SMP-17-010**
	dσ/dϕ*				EPJC76(2016)291 JHEP03(2018)172	**CMS-PAS-SMP-17-010**
	Ai/AFB				JHEP08(2016)159 EPJC78(2018)701 PLB750(2015)154	
	sin2θW				ATLAS-CONF-2018-037 EPJC78(2018)701	

(*) in Elena Yatsenko's talk

Z at 13 TeV

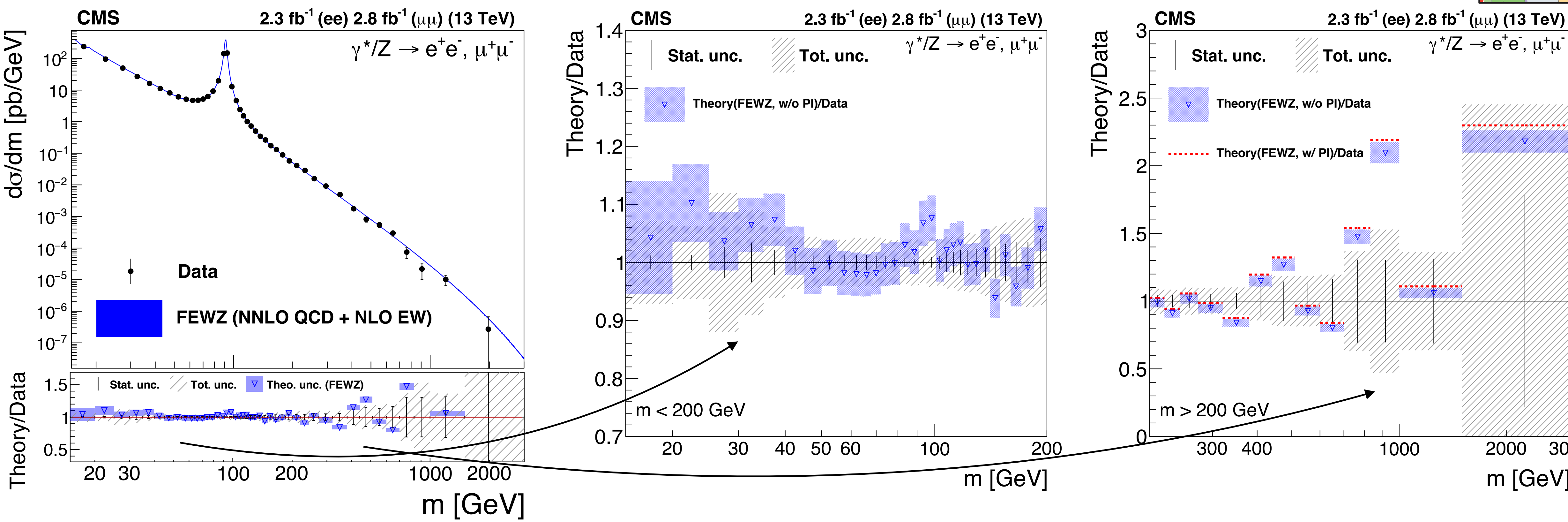

- $d\sigma/dm$ of Z cross section with 2.3-2.8 fb^{-1} at 13 TeV (2015)
  - fiducial selection (leptons after FSR) for $Z\rightarrow\mu\mu$(ee): p_T^l>22(30),10GeV, $|\eta_l|$<2.4(2.5)
  - cross sections in full lepton phase space corrected for FSR effects (dressed leptons)
- Full phase space cross sections in good agreement with FEWZ(NNLO QCD + NLO EW) with NNPDF3.0
  - predictions with photon-induced contributions also tested at high m_{ll} with FEWZ+LUXqed

arXiv:1812.10529 (sub. to JHEP)

Z at 13 TeV

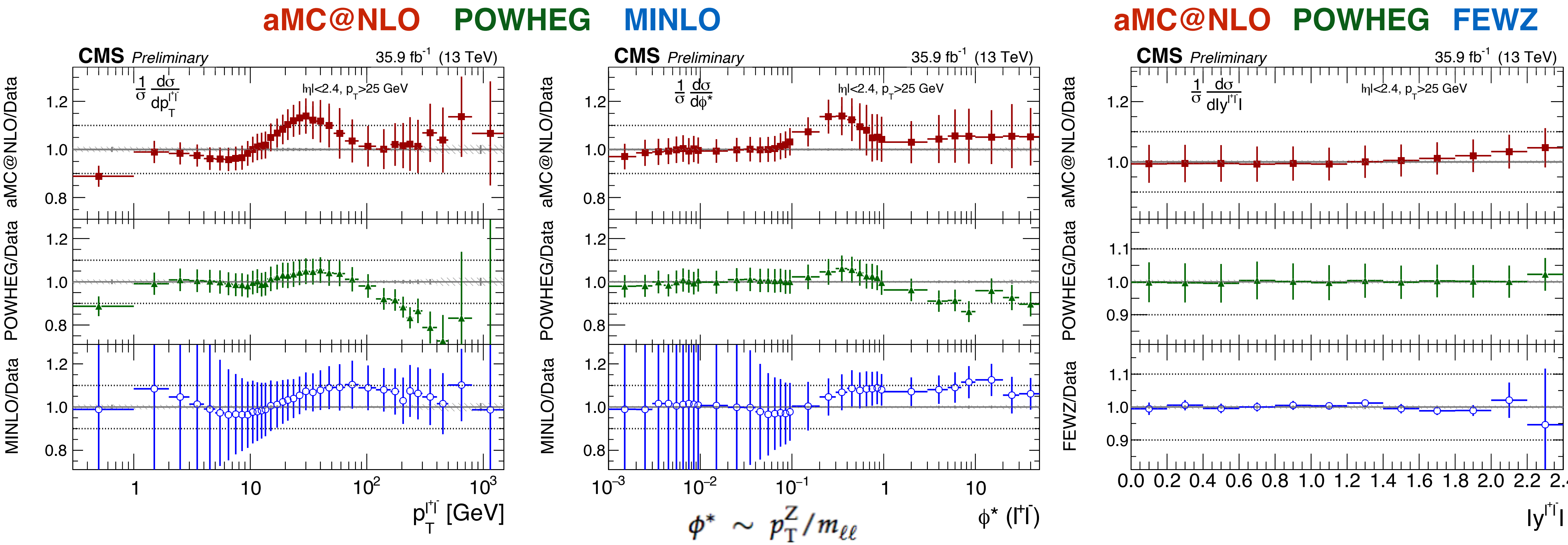

- p_T^{ll}, ϕ^*, y^{ll} differential Z cross section in ee,$\mu\mu$ events at 13 TeV with 35.9 fb^{-1} (also 2D p_T^{ll}-y^{ll} differential cross section)
  - fiducial selection: fiducial selection (leptons after FSR): p_T^l>25 GeV, $|\eta|$<2.4, $|m_{ll}$-91.2$|$<15 GeV
- Normalised cross section uncertainties smaller than 0.5% for p_T^{ll}<50 GeV
- Measurements compared fixed-order, resummed and parton shower predictions
  - FO: Z at NNLO QCD (FEWZ) and Z+j at NNLO QCD (ZjNNLO). LO EW
  - Resummed (NNLL): Geneva, Resbos
  - PS: MadGraph5_aMC@NLO (0,1,2j at NLO, FxFx), Powheg (NLO), Powheg+MiNLO (0,1j at NLO)

Z at 13 TeV

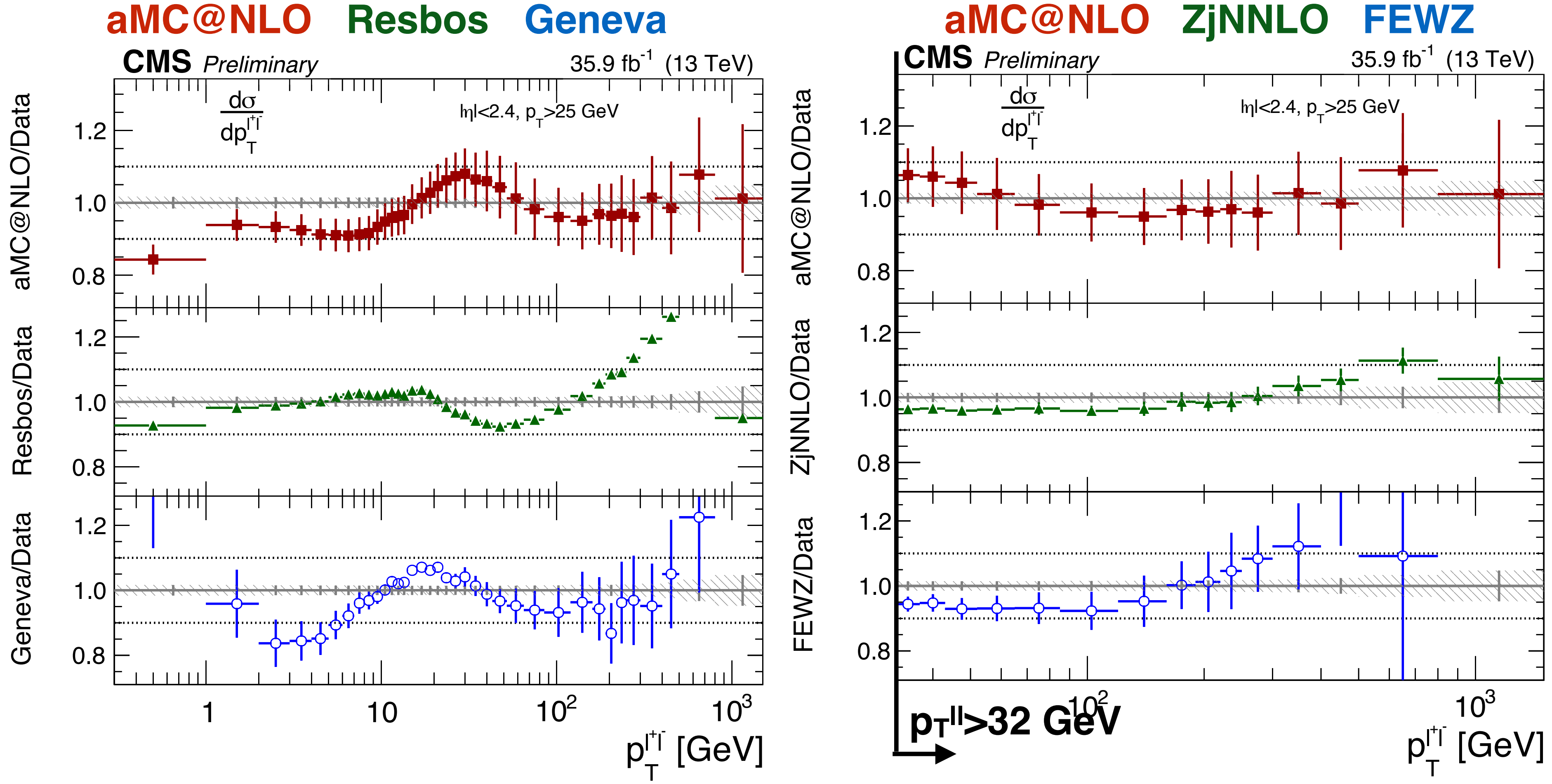

- p_T^{ll}, ϕ^*, y^{ll} differential Z cross section in ee,$\mu\mu$ events at 13 TeV with 35.9 fb^{-1} (also 2D p_T^{ll}-y^{ll} differential cross section)
  - fiducial selection: fiducial selection (leptons after FSR): p_T^l>25 GeV, $|\eta|$<2.4, $|m_{ll}$-91.2|<15 GeV
- Normalised cross section uncertainties smaller than 0.5% for p_T^{ll}<50 GeV
- Measurements compared fixed-order, resummed and parton shower predictions
  - FO: Z at NNLO QCD (FEWZ) and Z+j at NNLO QCD (ZjNNLO). LO EW
  - Resummed (NNLL): Geneva, Resbos
  - PS: MadGraph5_aMC@NLO (0,1,2j at NLO, FxFx), Powheg (NLO), Powheg+MiNLO (0,1j at NLO)

W→$\mu\nu$ at 8 TeV

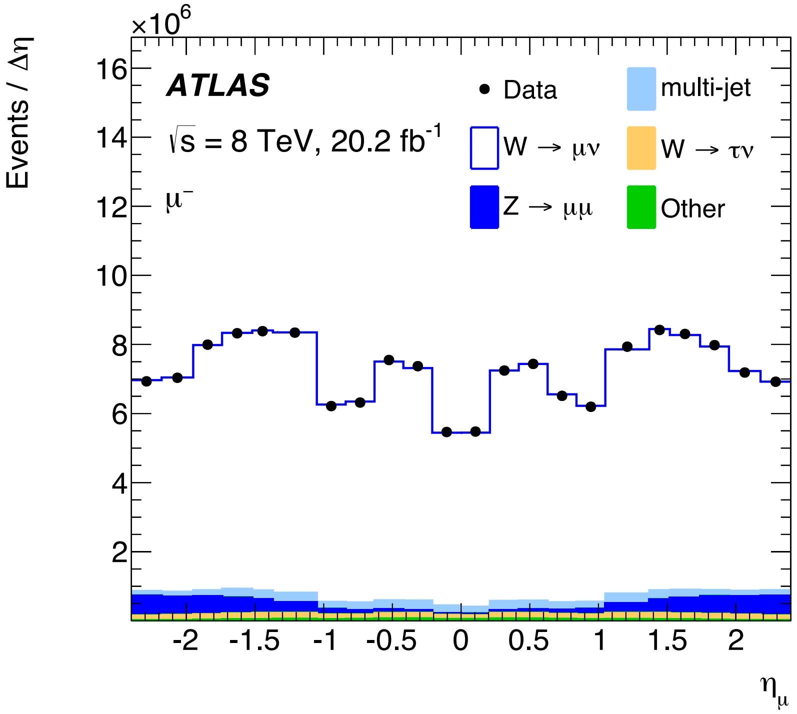

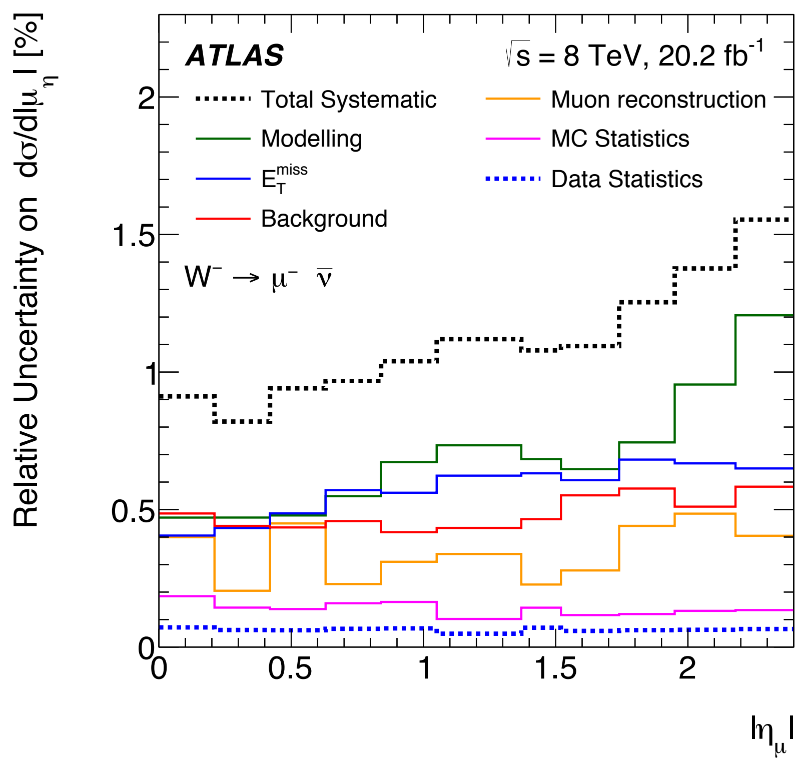

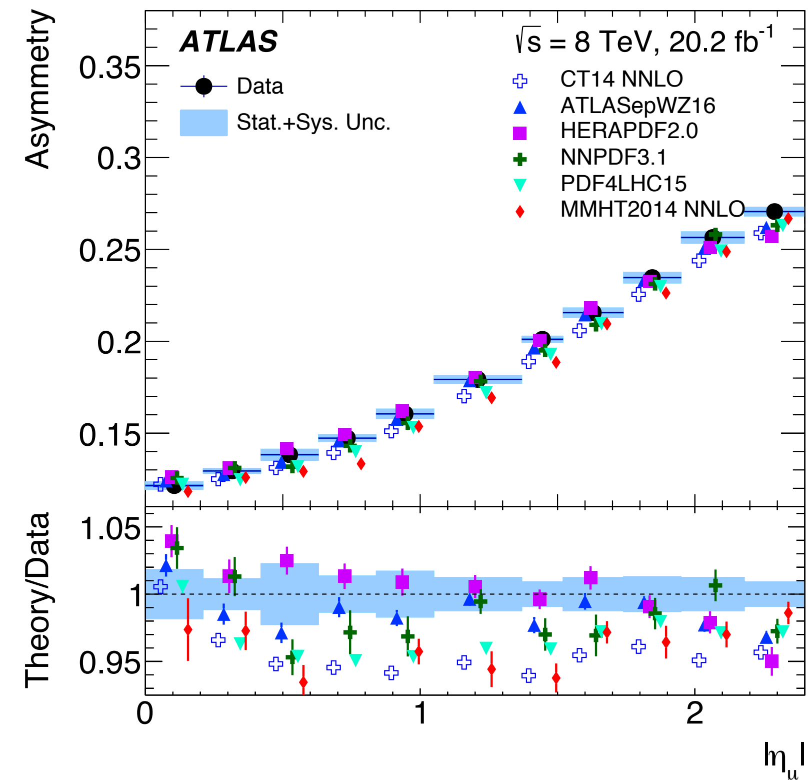

- $|\eta_\mu|$-differential fiducial W cross section and charge asymmetry
  - W→$\mu\nu$ events with 20 fb^{-1} of *pp* collisions at 8 TeV
  - results consistent with W→eν at 8TeV (JHEP05(2018)077)
  - fiducial selection (born lepton): p_T^μ>25 GeV, p_T^ν>25GeV, $|\eta_\mu|$<2.4, m_T>40GeV
- Dominant uncertainty from luminosity (1.9%), other uncertainties at ~0.5%
- Measurements compared to DYNNLO predictions with different PDF sets
  - data at 1% precision can discriminate among PDF sets

W,Z at 5 TeV

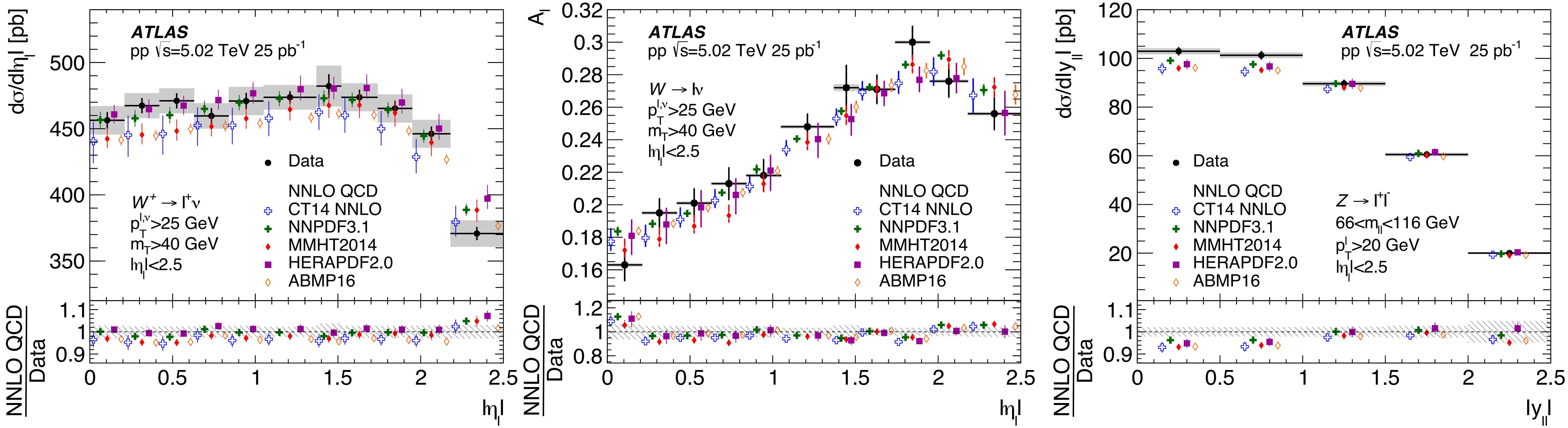

- Differential fiducial W±,Z cross sections and W charge asymmetry at 5.02 TeV
  - 25 pb^{-1} of *pp* collisions (reference for *PbPb* run)
  - fiducial selection (born leptons):
    - W: p_T^l>25 GeV, p_T^ν>25GeV, $|\eta|$<2.5, m_T>40GeV
    - Z: p_T^l>20 GeV, $|\eta|$<2.5, 66<m_{ll}<116GeV
- Dominant uncertainties from luminosity (1.9%) and lepton selection efficiencies
- Measurements (~2% precision) compared to DYNNLO predictions with different PDF sets
  - 1-2σ deviations, in particular in central y_{ll} (consistent with 7 TeV result EPJC77(2017)367)

Summary

$$\sin^2\theta_W = 1 - M_W^2/M_Z^2$$

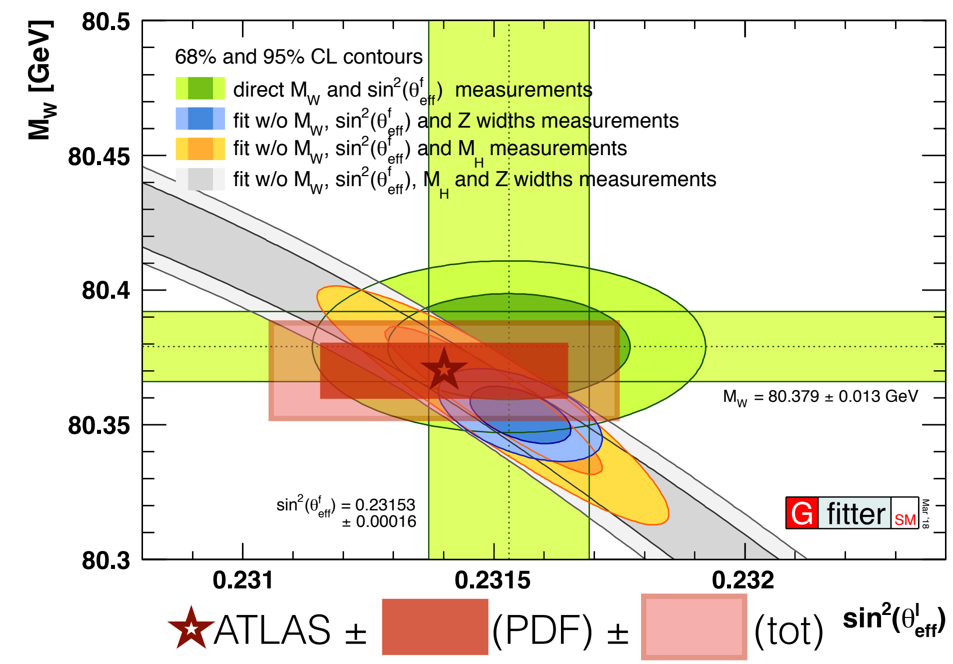

- LHC experiments reaching unprecedented precisions
  - accurate knowledge of detector at different energies and pileup conditions
  - individual LHC experiments at similar precision of combined LEP, SLD and Tevatron EW measurements
  - (multi-)differential W,Z cross sections at sub-percent precision
- Prediction uncertainties (PDFs) limiting factor in exploiting full LHC potential for EW measurements
- Experimental and theory communities working towards future measurements and combinations
  - studies of differences/correlations among PDF sets
  - studies of O(1%) corrections from EW, QED, HO and NP QCD effects and their correlations
  - better assessment of theory uncertainties
  - use of high-precision LHC data to improve knowledge of (non-)perturbative QCD and of proton structure

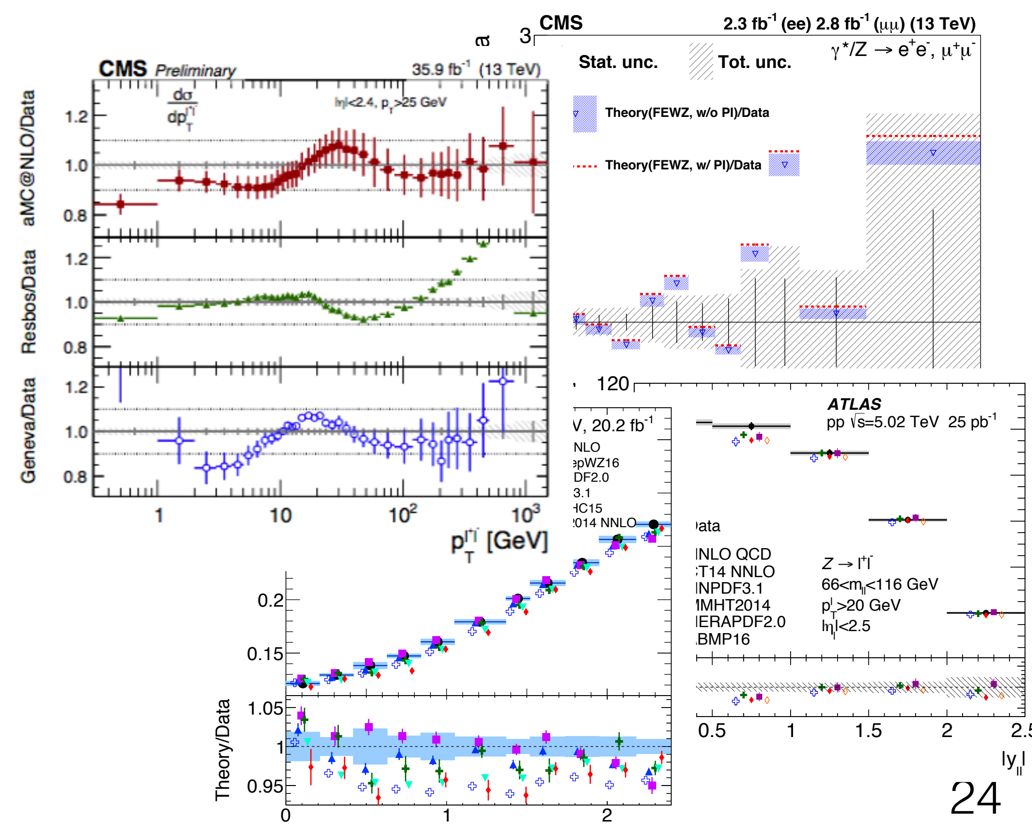

Additional Material

W mass and W pT

EPJC76(2016)291

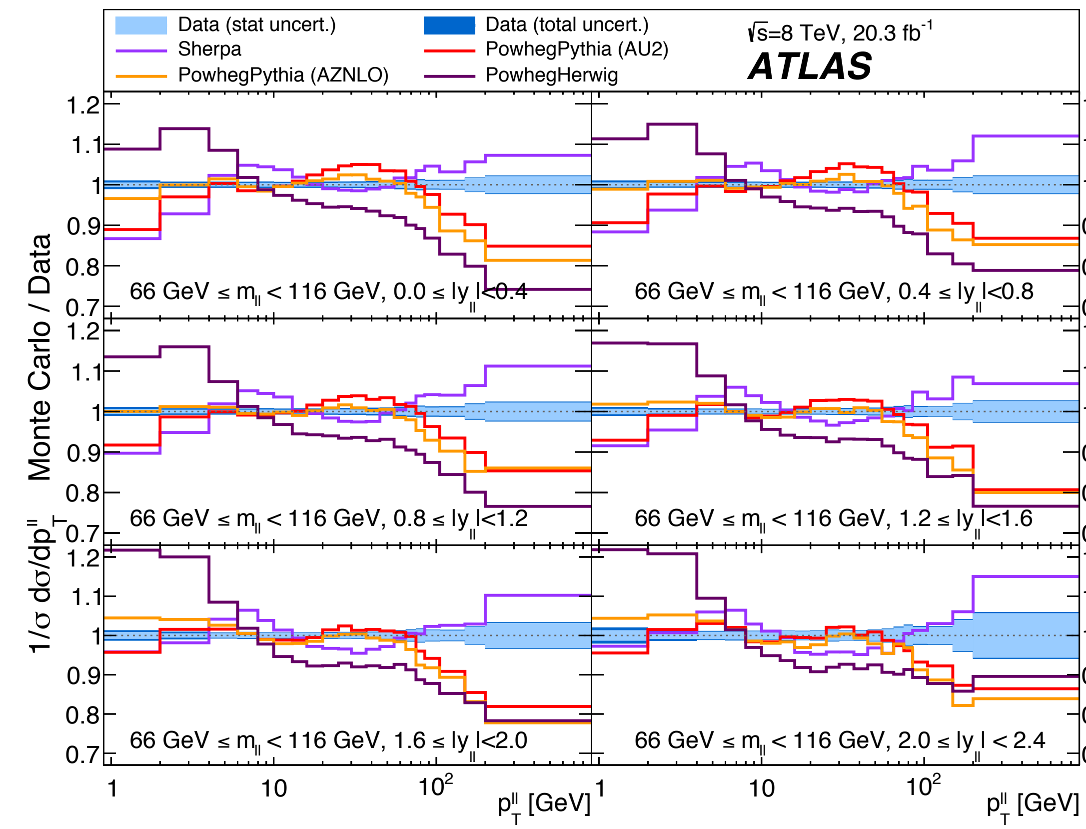

DYNNLO

$$\frac{d\sigma}{dp_1\,dp_2} = \left[\frac{d\sigma(m)}{dm}\right]\left[\frac{d\sigma(y)}{dy}\right]\left[\frac{d\sigma(p_T,y)}{dp_T\,dy}\left(\frac{d\sigma(y)}{dy}\right)^{-1}\right]\left[(1+\cos^2\theta)+\sum_{i=0}^{7}A_i(p_T,y)P_i(\cos\theta,\phi)\right]$$

$$\frac{d\sigma}{dm} \propto \frac{m^2}{(m^2-m_V^2)^2+m^4\Gamma_V^2/m_V^2}$$

Breit-Wigner

Pythia8 AZ

W-boson charge / Kinematic distribution	W^+ p_T^ℓ	W^+ m_T	W^- p_T^ℓ	W^- m_T	Combined p_T^ℓ	Combined m_T
δm_W [MeV]						
Fixed-order PDF uncertainty	13.1	14.9	12.0	14.2	8.0	8.7
AZ tune	3.0	3.4	3.0	3.4	3.0	3.4
Charm-quark mass	1.2	1.5	1.2	1.5	1.2	1.5
Parton shower μ_F with heavy-flavour decorrelation	5.0	6.9	5.0	6.9	5.0	6.9
Parton shower PDF uncertainty	3.6	4.0	2.6	2.4	1.0	1.6
Angular coefficients	5.8	5.3	5.8	5.3	5.8	5.3
Total	15.9	18.1	14.8	17.2	11.6	12.9

☐ = PDF syst, the rest are QCD syst

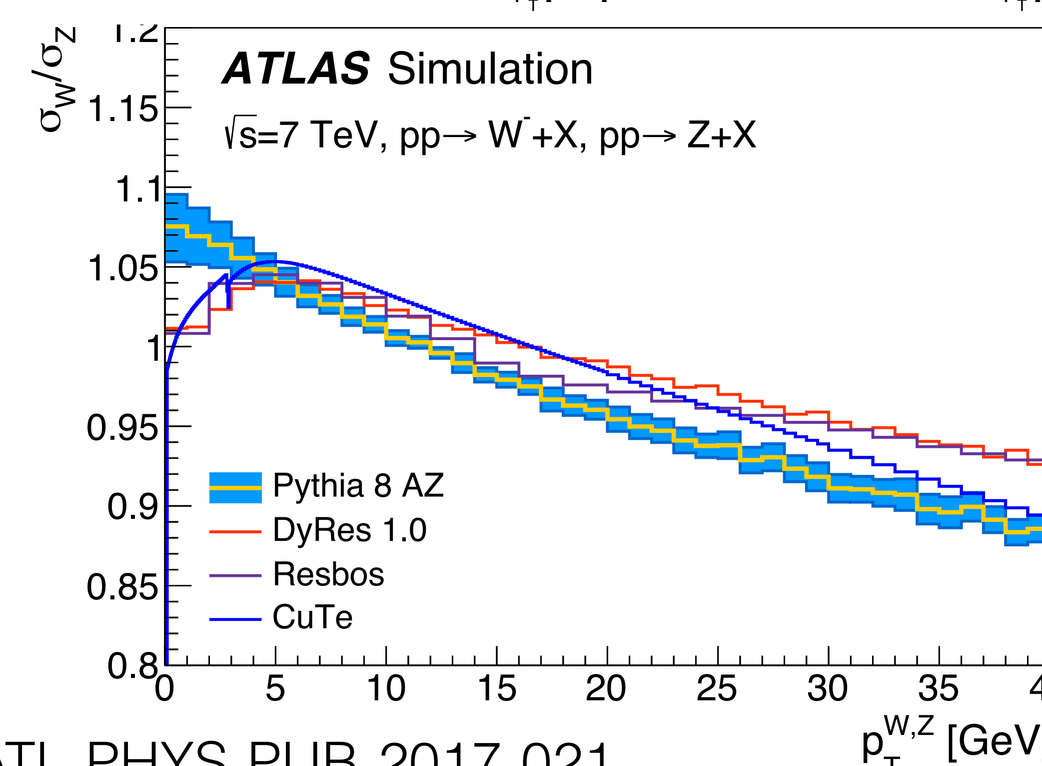

ATL-PHYS-PUB-2017-021

p_T^W Prospects

- Improved N3LL+NNLO predictions?
  - preferable to MC tunes which cannot model all corners of phase space and are not expected to scale properly with energy
  - MC tunes at <1% precision to be handled with care to avoid unphysical correlations
- Promising results, but 1% uncertainty won't be reached soon
  - currently good agreement with data in different eta/mass bins at 5% precision
  - uncertainty on W/Z ratio depends a lot on correlation scheme (not yet established)
- LHC W,Z measurements, at low and high μ, will help improving predictions (p_T^W, UE, PDF) and
  - study mechanisms responsible for differences in Z and W pTs (eg HF initial state partons)
  - energy dependence in p_T modelling
- Efforts ongoing in benchmarking resummed calculations within LHC EW precision group

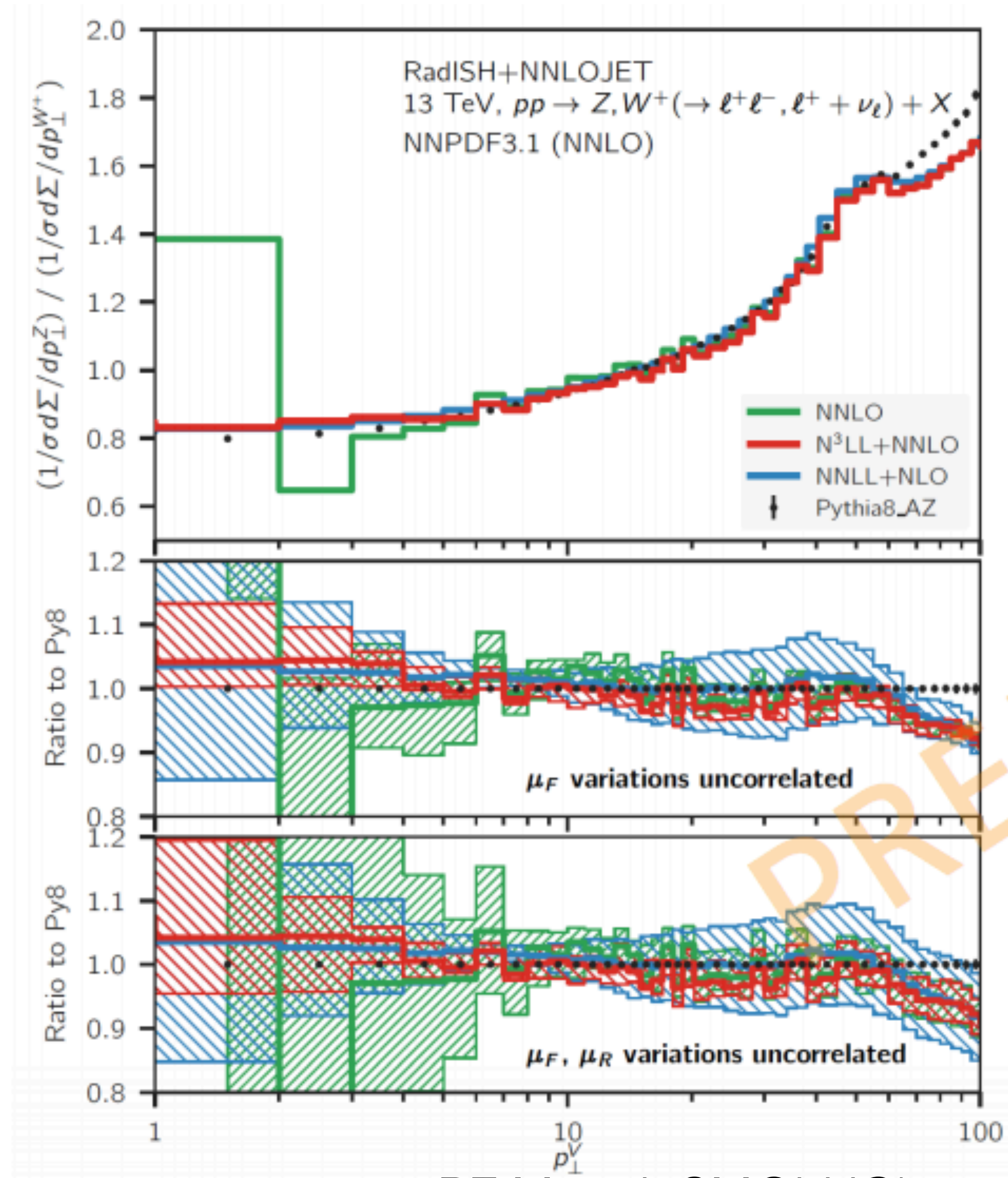

PF Monni, SM@LHC'19

sin2θW

- Z boson couplings differ between L- and R-handed leptons and this leads to an asymmetry in the angular distributions of charged leptons from Z decays
- This asymmetry depends on the weak mixing angle sin2θW that is the relative coupling strengths between photon and Z boson
- Differential LO cross section $Z/\gamma^* \to ll$ decay (θ is angle between lepton and quark, s is q/q CoME)
- Asymmetric term B generated by $\chi 1$ interference between Z and γ^* (proportional to couplings not dependent on sin2θW) and $\chi 2$ Z Breit-Wigner (with vector couplings proportional to sin2θW)
- Experimental asymmetry AFB (θ^* is angle between negative lepton and quark in Collin-Soper frame) depends directly on axial and vector couplings, and on sin2θW that relates the two
  - in decay lepton full phase space AFB=3/8A4

$$\sin^2\theta_{OS} = 1 - \frac{m_W^2}{m_Z^2}$$

on shell definition, valid at all orders

$$\sin^2\theta^l_{eff} = (1 - \frac{m_W^2}{m_Z^2}) K_Z^l$$

$$\frac{d\sigma}{d(\cos\theta)} = \frac{\alpha^2}{4s}\left[\frac{3}{8}A(1+\cos^2\theta) + B\cos\theta\right]$$

$$A = Q_l^2 Q_q^2 - 2Q_l g_V^q g_V^l \chi_1 + ({g_A^q}^2 + {g_V^q}^2)({g_A^l}^2 + {g_V^l}^2)\chi_2 ,$$
$$B = -4Q_l g_A^q g_A^l \chi_1 + 8 g_A^q g_V^q g_A^l g_V^l \chi_2 ,$$
$$g_A^f = t_3^f$$
$$g_V^f = t_3^f - (2Q_f \times \sin^2\theta_W)$$

$$A_{FB} = \frac{N(\cos\theta^* > 0) - N(\cos\theta^* < 0)}{N(\cos\theta^* > 0) + N(\cos\theta^* < 0)} = \frac{3}{8}\frac{B}{A}$$

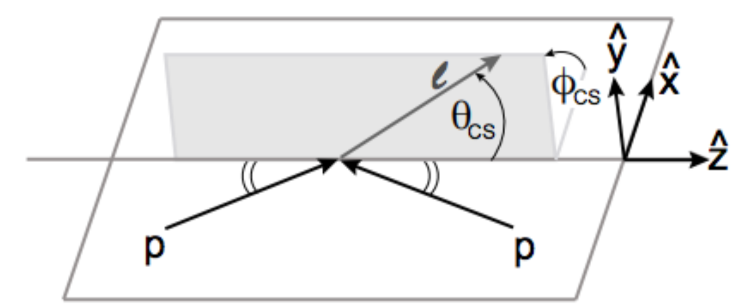

sin2θW

- A_{FB},A_4 arise from
  - Z/γ^* interference (strongly mll dependent)
  - Z coupling (sensitive to $\sin^2\theta^f_{eff}$ and constant in mll, no need for fine binning in m^{ll})
- Asymmetries dependent on quark flavours and dilution effect

LO EW NLO+HO EW

$A_4 = a^*\sin^2\theta_W + b \rightarrow (a+\delta a_{EW})^*\sin^2\theta^l_{eff} + (b+\delta b_{EW})$

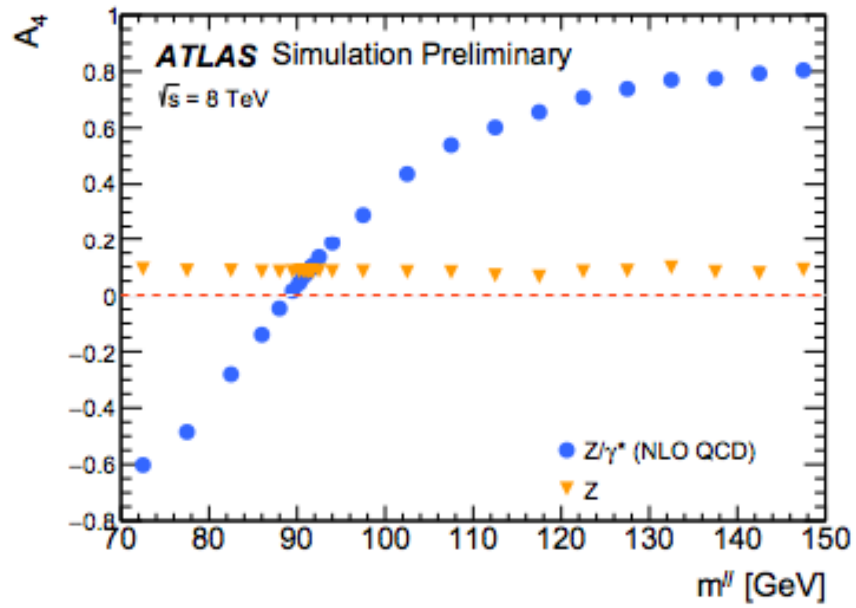

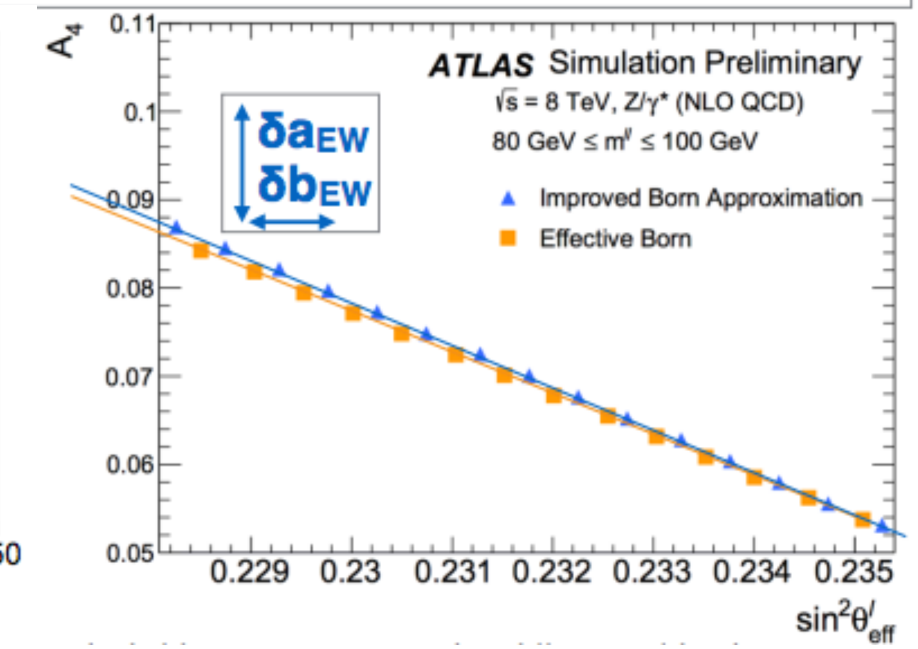

ATLAS-CONF-2018-037

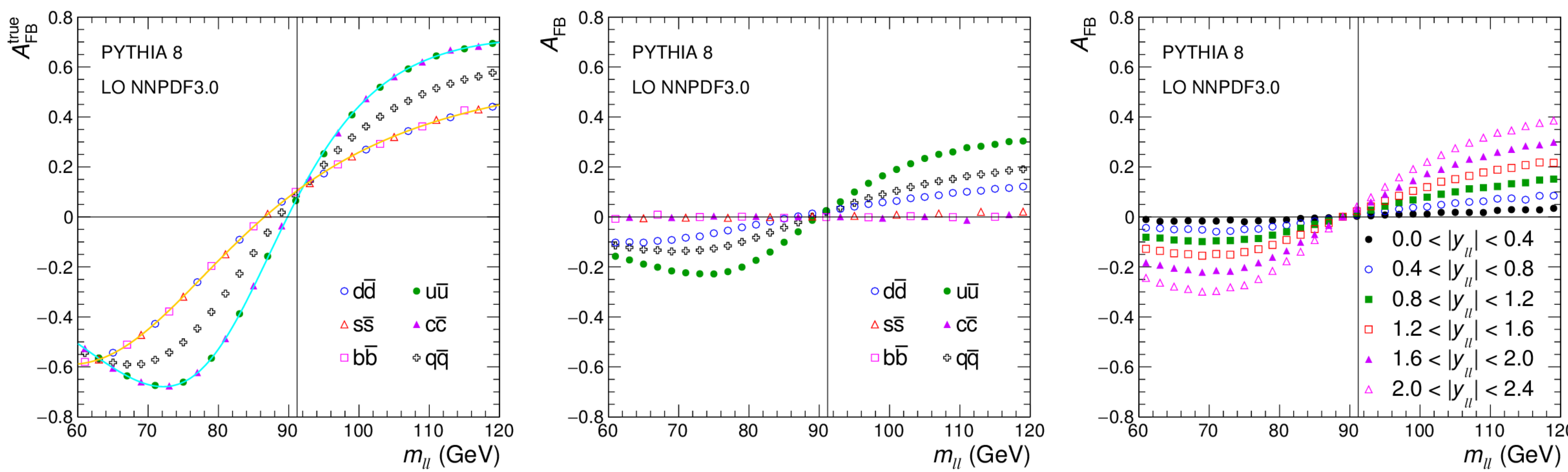

Ai vs Z3D

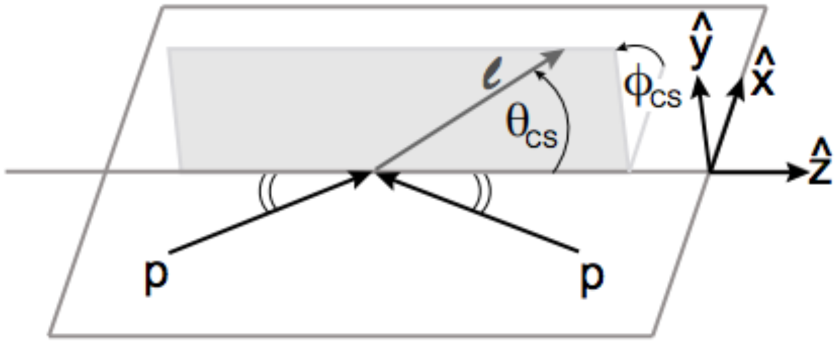

$$\frac{d\sigma}{dp_T^{\ell\ell}\, dy^{\ell\ell}\, dm^{\ell\ell}\, d\cos\theta\, d\phi} = \frac{3}{16\pi} \frac{d\sigma^{U+L}}{dp_T^{\ell\ell}\, dy^{\ell\ell}\, dm^{\ell\ell}} \Big\{(1+\cos^2\theta) + \frac{1}{2} A_0(1-3\cos^2\theta) + A_1 \sin 2\theta \cos\phi + \frac{1}{2} A_2 \sin^2\theta \cos 2\phi + A_3 \sin\theta \cos\phi + A_4 \cos\theta + A_5 \sin^2\theta \sin 2\phi + A_6 \sin 2\theta \sin\phi + A_7 \sin\theta \sin\phi\Big\}.$$

- Advantages of harmonic decomposition compared to fiducial cross section measurement
  - can constraint experimental systematics
  - extrapolation to full phase space reduces theory systematics and allows for channel-to-channel comparison without extrapolation
- Cons: more sensitive to NLO EW corrections (including boxes) that can break decomposition
- More details in https://indico.cern.ch/event/749003/contributions/3329387/attachments/1826179/2988810/armbruster.pdf

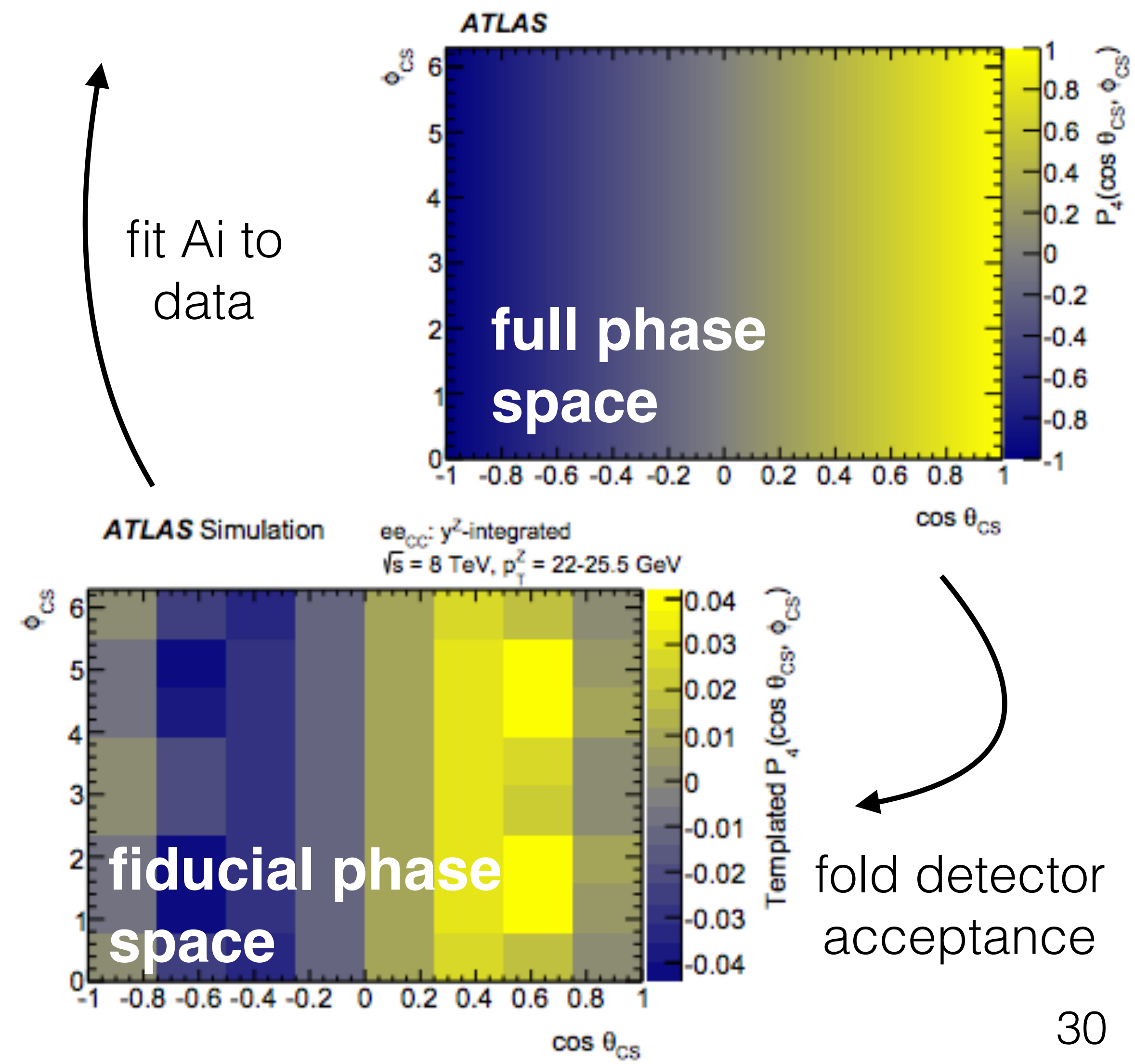

EW Corrections

~Linear relation between A_4 and $\sin^2\theta^l_{eff}$

LO EW	NLO+HO EW
$A_4 = a*\sin^2\theta_W + b$	$\rightarrow (a+\delta a_{EW})*\sin^2\theta^l_{eff} + (b+\delta b_{EW})$

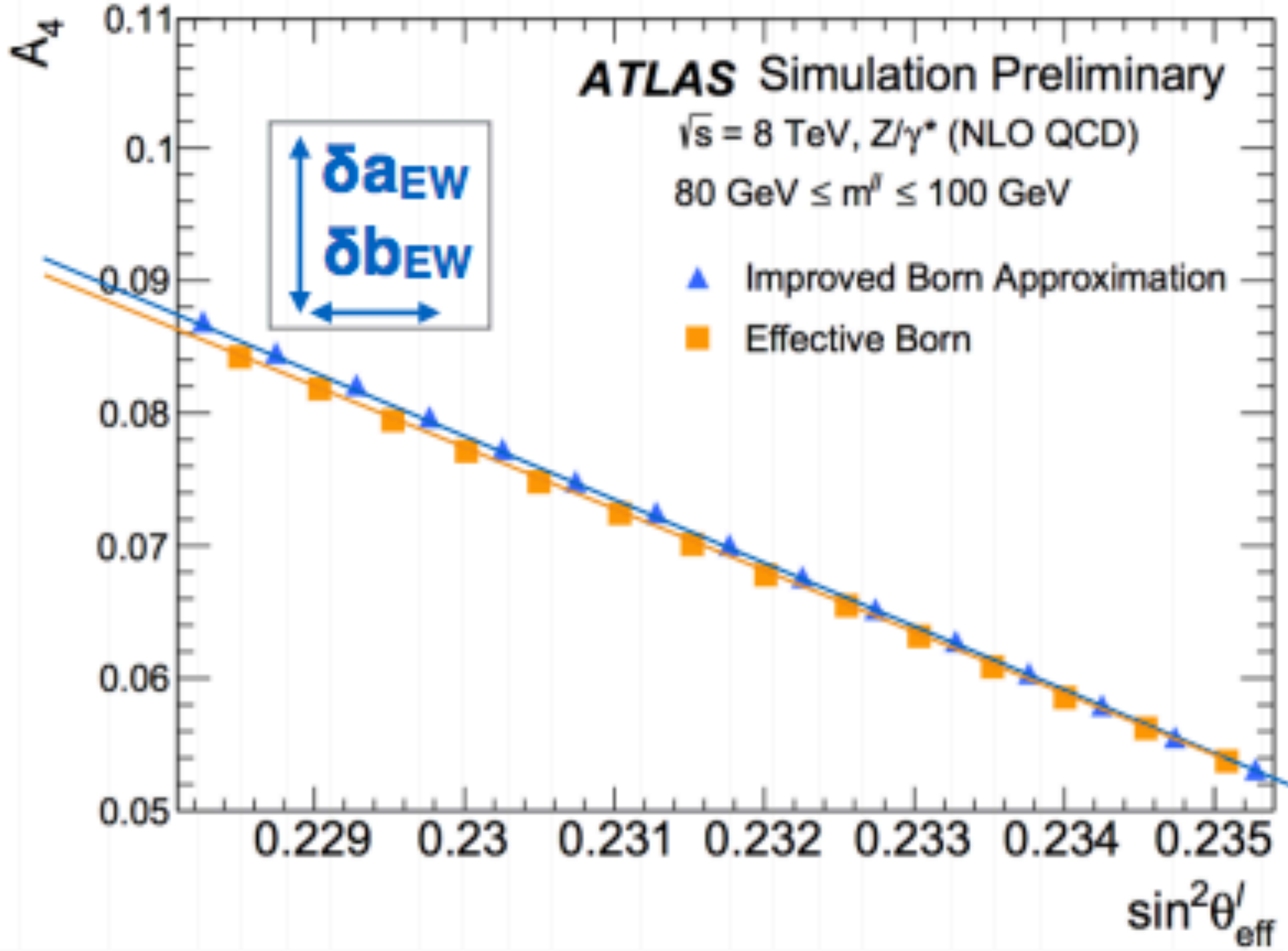

$v_f = (2*T^f_3 - 4*q_f*\sin^2\theta_W \cdot \mathbf{K^f(s,t)})/\Delta$

- Compute form factors $K^f(s,t)$ using DIZET libraries
- Define *effective leptonic* WMA at $s=m^Z$
  - $\sin^2\theta^{lep}_{eff} = \sin^2\theta_W * K^{lep}(m^Z)$

$v_f = (2*T^f_3 - 4*q_f*(\sin^2\theta_W \cdot K^f(s,t) \mathbf{+\delta v}))/\Delta$

- Scan $\sin^2\theta^{lep}_{eff}$ in predictions by scanning equivalent shift in coupling term
- Compute correction δa_n^{EW}, δb_n^{EW} and add to LO EW predictions to obtain scan vs $\sin^2\theta^{lep}_{eff}$
- Results in ~**25 * 10^{-5}** shift in measurement

- A. Armbruster at DIS2019 (link)

Ai Results

eeCC

$\|y_{ll}\|$	Data	Top+EW	Multijets	Non-fiducial Z
	$70 < m_{ll} < 80$ GeV			
0-0.8	106 718	0.023	0.015	0.010
0.8-1.6	95 814	0.015	0.020	0.010
1.6-2.5	47 078	0.012	0.041	0.009
	$80 < m_{ll} < 100$ GeV			
0-0.8	2 697 316	0.003	0.001	< 0.001
0.8-1.6	2 084 856	0.002	0.001	< 0.001
1.6-2.5	839 424	0.002	0.002	< 0.001
	$100 < m_{ll} < 125$ GeV			
0-0.8	106 855	0.034	0.016	0.023
0.8-1.6	80 403	0.025	0.019	0.027
1.6-2.5	28 805	0.015	0.025	0.029

mmCC

$\|y_{ll}\|$	Data	Top+EW	Multijets	Non-fiducial Z
	$70 < m_{ll} < 80$ GeV			
0-0.8	124 050	0.019	0.017	0.009
0.8-1.6	137 984	0.015	0.014	0.014
1.6-2.5	74 976	0.010	0.011	0.019
	$80 < m_{ll} < 100$ GeV			
0-0.8	2 866 016	0.002	0.001	< 0.001
0.8-1.6	2 948 371	0.002	0.001	< 0.001
1.6-2.5	1 314 890	0.002	0.001	< 0.001
	$100 < m_{ll} < 125$ GeV			
0-0.8	119 650	0.030	0.023	0.023
0.8-1.6	122 775	0.020	0.015	0.023
1.6-2.5	55 886	0.010	0.005	0.022

eeCF

$\|y_{ll}\|$	Data	Top+EW	Multijets	Non-fiducial Z
	$80 < m_{ll} < 100$ GeV			
1.6-2.5	702 142	0.001	0.010	0.017
2.5-3.6	441 104	0.001	0.011	0.013

Ai Control Plots

- Good modelling of angular distributions between data and MC “prefit”
- Angular coefficients measured in-situ → theory modelling corrected within fit
- Very high and very low |cosθ| regions in eeCF related to pTZ modelling
  - little impact on measured sin2θW, covered by systematics
- Large lever-arm in eeCF channel: contributes to superiority of channel

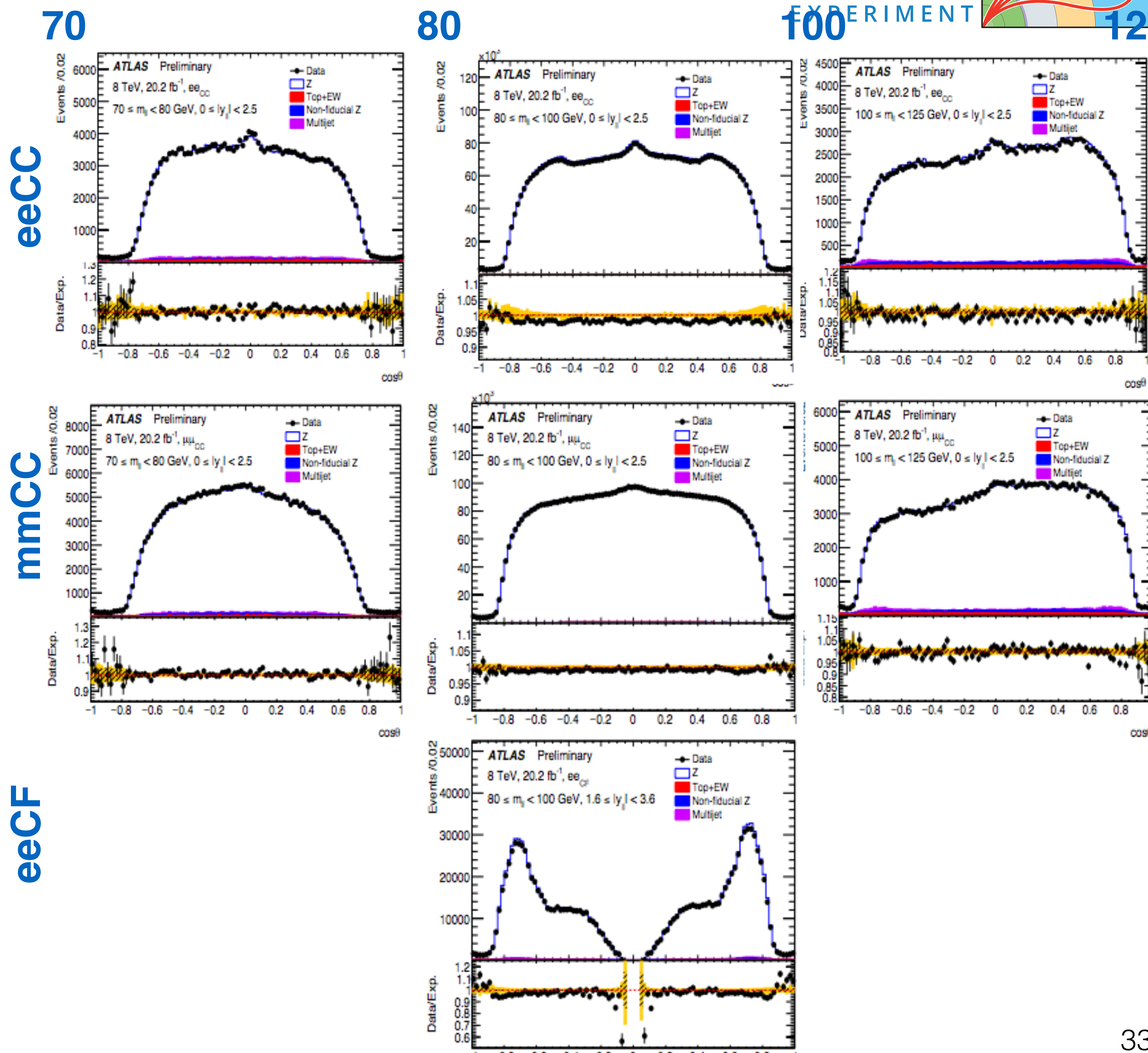

CMS sin2θW

$$\frac{1}{\sigma}\frac{d\sigma}{d\cos\theta^*} = \frac{3}{8}\left[1+\cos^2\theta^* + \frac{A_0}{2}(1-3\cos^2\theta^*) + A_4\cos\theta^*\right]$$

The A_{FB} value in each $(m_{\ell\ell}, y_{\ell\ell})$ bin is calculated using the "angular event weighting" method, described in Ref. [40], in which each event with a $\cos\theta^*$ value (denoted as "c"), is reflected in the denominator (D) and numerator (N) weights through:

$$w_D = \frac{1}{2}\frac{c^2}{(1+c^2+h)^3}, \tag{8}$$

$$w_N = \frac{1}{2}\frac{|c|}{(1+c^2+h)^2}, \tag{9}$$

where $h = 0.5A_0(1-3c^2)$. Here, as a baseline we use the $p_{T,\ell\ell}$-averaged A_0 value of about 0.1 in each measurement $(m_{\ell\ell}, y_{\ell\ell})$ bin, as predicted by the signal MC simulation. Using the weighted sums N and D for forward ($\cos\theta^* > 0$) and backward ($\cos\theta^* < 0$) events, we obtain

$$D_F = \sum_{c>0} w_D, \quad D_B = \sum_{c<0} w_D, \tag{10}$$

$$N_F = \sum_{c>0} w_N, \quad N_B = \sum_{c<0} w_N, \tag{11}$$

from which the weighted A_{FB} of Eq. (2) can be written as:

$$A_{FB} = \frac{3}{8}\frac{N_F - N_B}{D_F + D_B}. \tag{12}$$

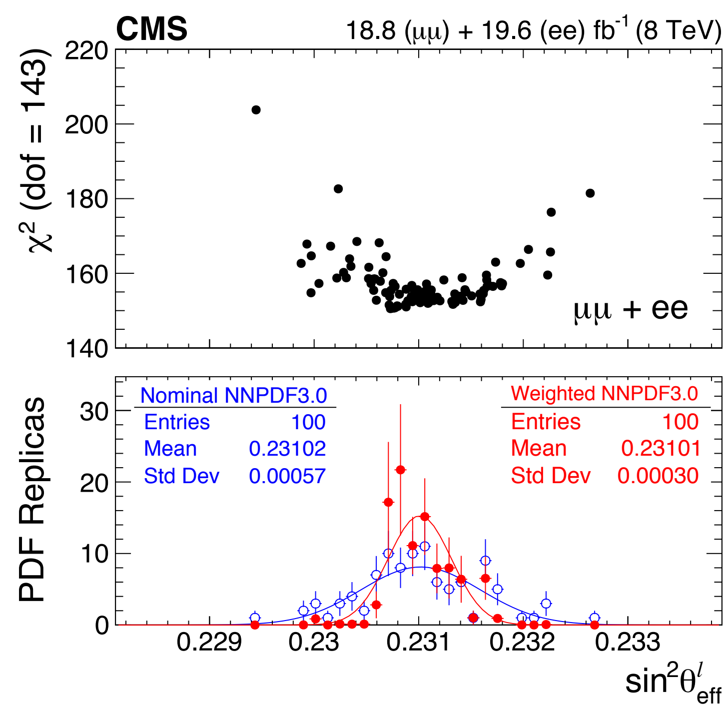

Source	Muons	Electrons
Size of MC event sample	0.00015	0.00033
Lepton selection efficiency	0.00005	0.00004
Lepton momentum calibration	0.00008	0.00019
Background subtraction	0.00003	0.00005
Modeling of pileup	0.00003	0.00002
Total	0.00018	0.00039

Modeling parameter	Muons	Electrons
Dilepton p_T reweighting	0.00003	0.00003
μ_R and μ_F scales	0.00011	0.00013
POWHEG MINLO Z+j *vs.* Z at NLO	0.00009	0.00009
FSR model (PHOTOS *vs.* PYTHIA 8)	0.00003	0.00005
Underlying event	0.00003	0.00004
Electroweak $\sin^2\theta^\ell_{eff}$ *vs.* $\sin^2\theta^{u,d}_{eff}$	0.00001	0.00001
Total	0.00015	0.00017

Channel	Statistical uncertainty
Muons	0.00044
Electrons	0.00060
Combined	0.00036

Channel	Not constraining PDFs	Constraining PDFs
Muons	0.23125 ± 0.00054	0.23125 ± 0.00032
Electrons	0.23054 ± 0.00064	0.23056 ± 0.00045
Combined	0.23102 ± 0.00057	0.23101 ± 0.00030

$\sin^2\theta_W$ PDF uncert

- As measurement performed in mZ and yZ bins, PDF correlation patterns are important in final impact of PDF syst on measurement
  - PDF and sin2θW correlations very different in mll
- Correlations exploited to reduce PDF syst by constraints to data

EPJC78(2018)701

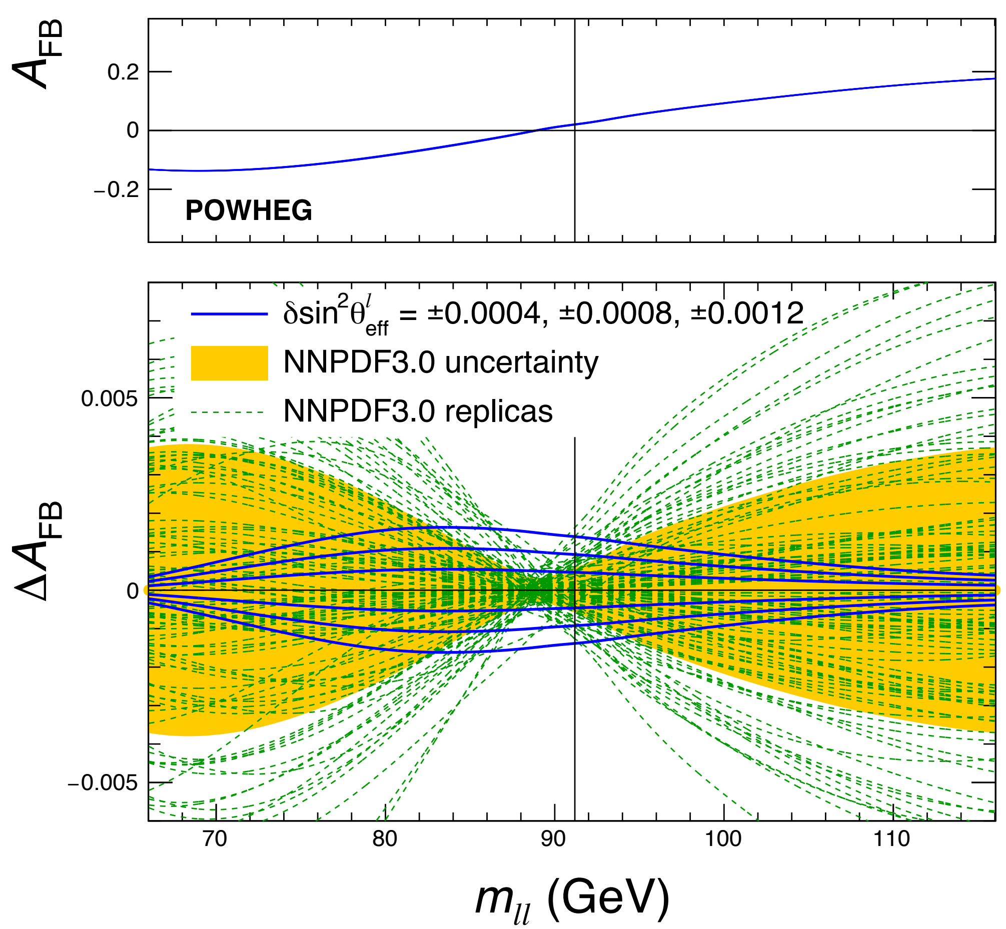

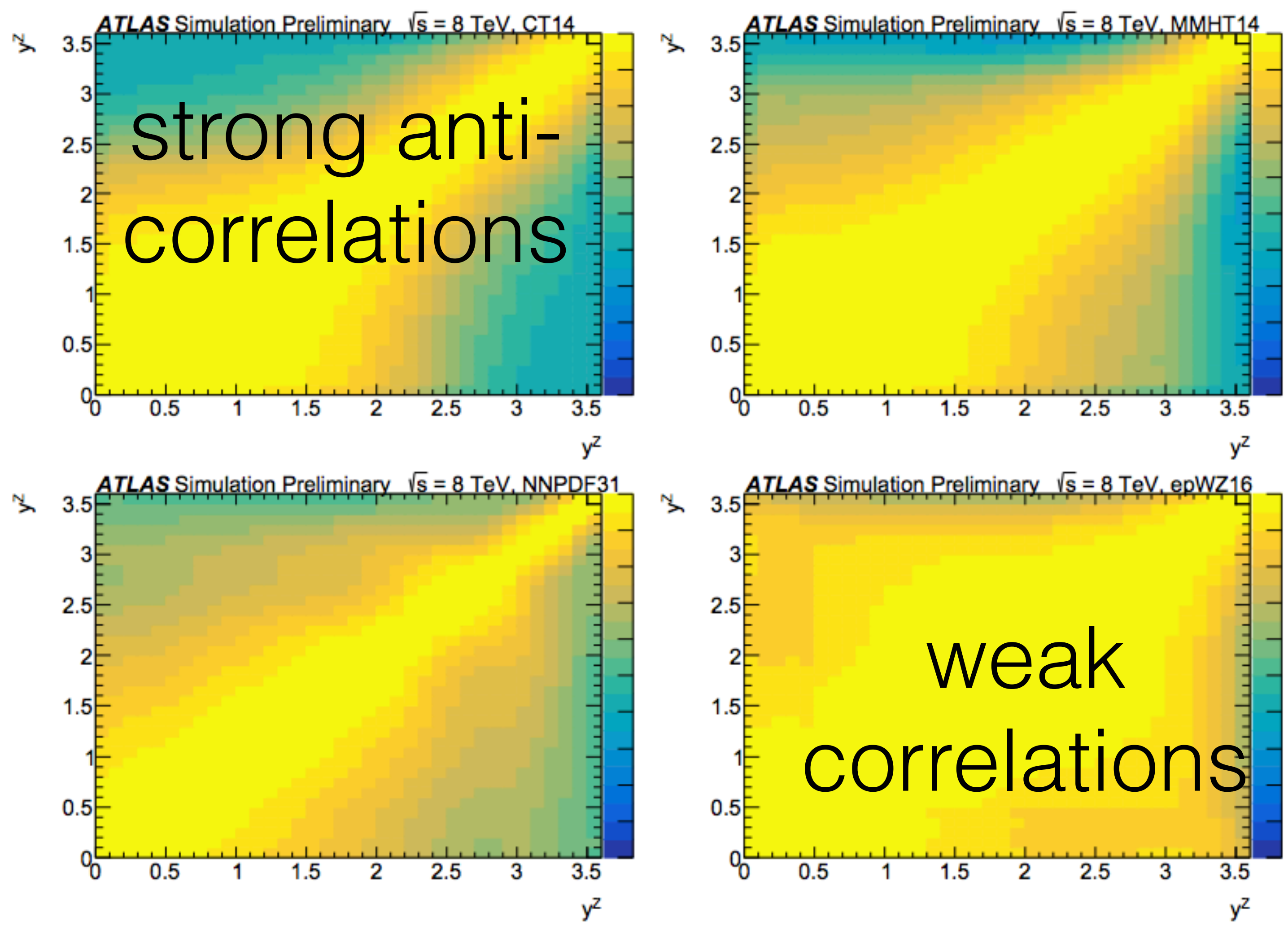

Figure 4: Correlations between the predicted angular coefficient A_4 as a function of y^Z, shown for the CT14 (top left), MMHT14 (top right), NNPDF31 (bottom left), and ATLAS epWZ16 (bottom right) PDF sets. The colour scale runs over the whole range from +1 (yellow) to −1 (blue).

ATL-PHYS-PUB-2018-004

$\sin^2\theta_W$ PDF Closure

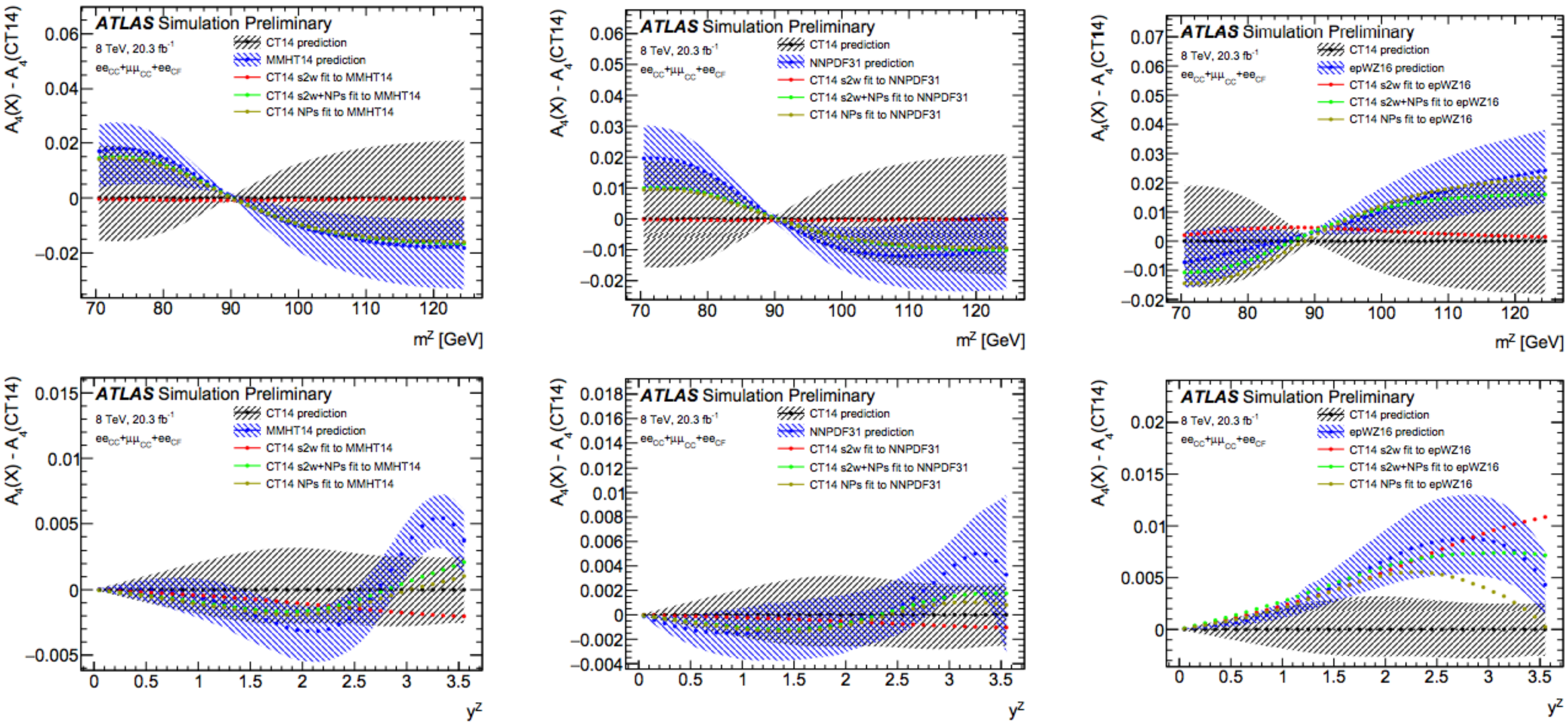

- Fit closes well in mll since variations in A4 from sin2θW and PDF are different
- Although with uncertainties, fit not closing in yll, possibly because of course analysis yll-bins and low stat at high yll

$\sin^2\theta_W$ PDF Closure

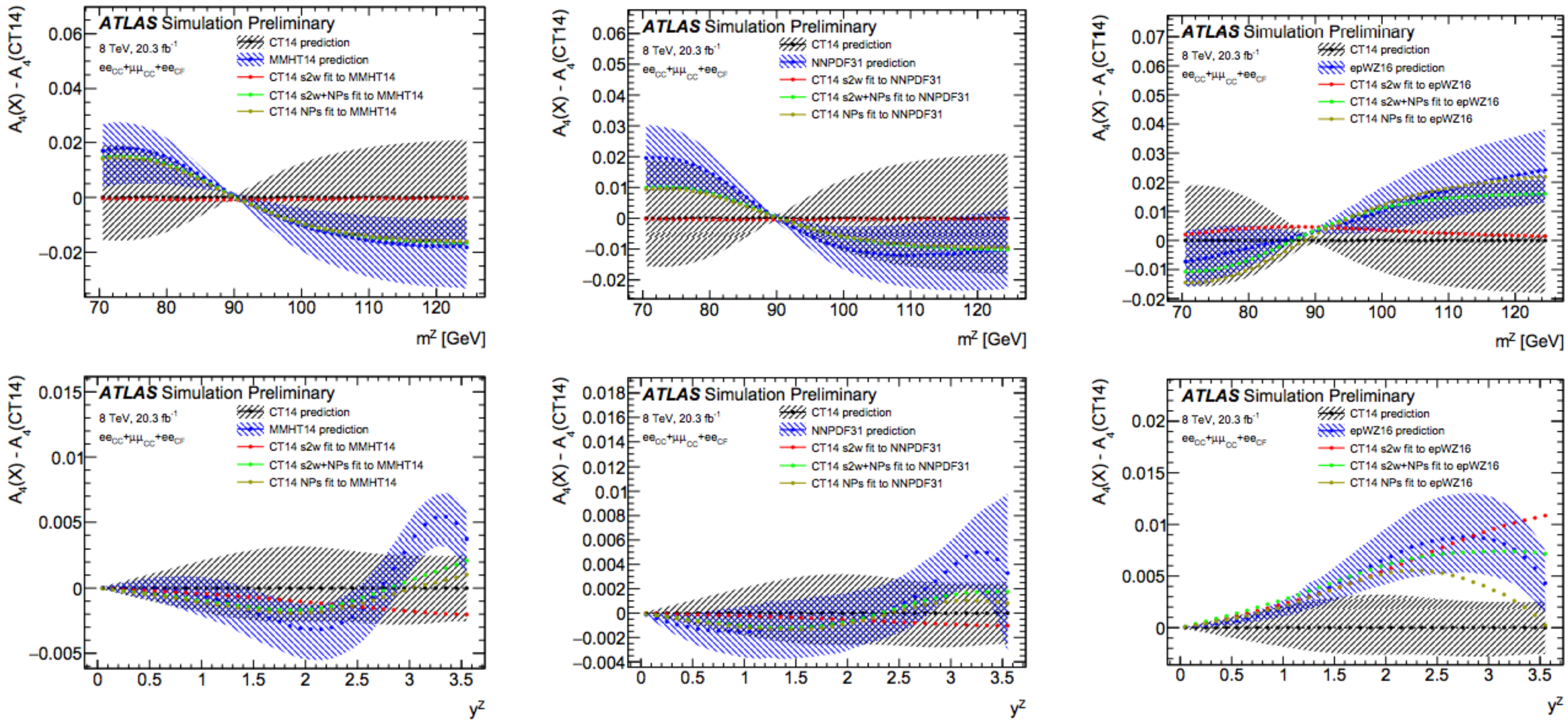

Generated pseudodata	PDFs used for interpretation of A4 versus $\sin^2\theta_W$									
	Before PDF constraint					After PDF constraint				
	CT10	CT14	MMHT14	NNPDF31	epWZ16	CT10	CT14	MMHT14	NNPDF31	epWZ16
CT10	-	20	2	11	109	-	3	19	19	52
CT14	-20	-	-18	-9	91	8	-	21	21	56
MMHT14	-1	18	-	9	108	-25	-11	-	1	31
NNPDF31	-10	9	-9	-	99	-14	-9	4	-	43
epWZ16	-116	-95	-114	-105	-	-44	-66	-42	-42	-

- differences mostly within 1σ PDF uncertainties (except for epWz16)
- expected statistical uncertainty of ~20x10^{-5}

Z at 13TeV

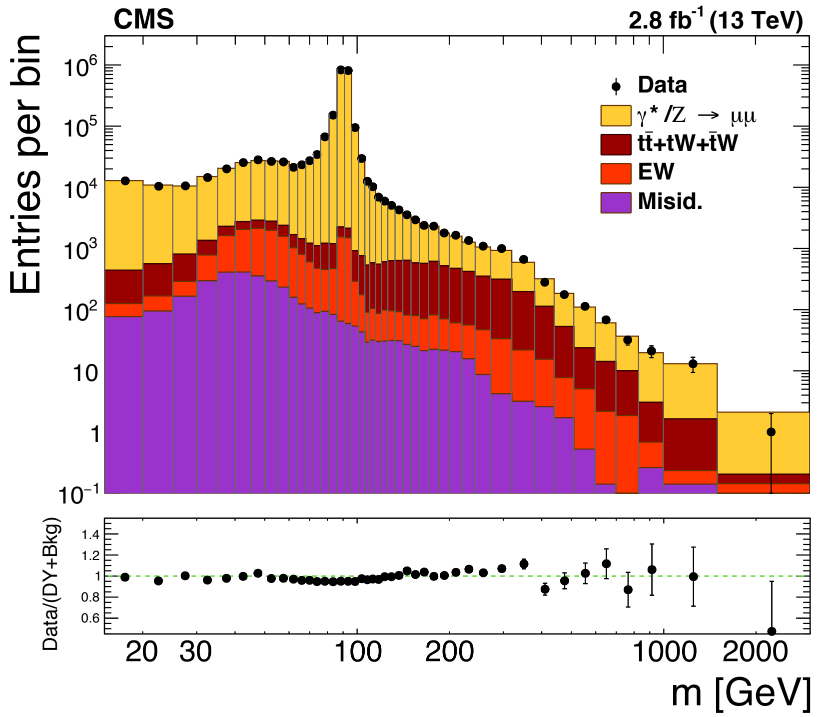
CMS
2.8 fb^{-1} (13 TeV)
Entries per bin
Data
$\gamma^*/Z \to \mu\mu$
$t\bar{t}$+tW+$\bar{t}$W
EW
Misid.
Data/(DY+Bkg)
m [GeV]

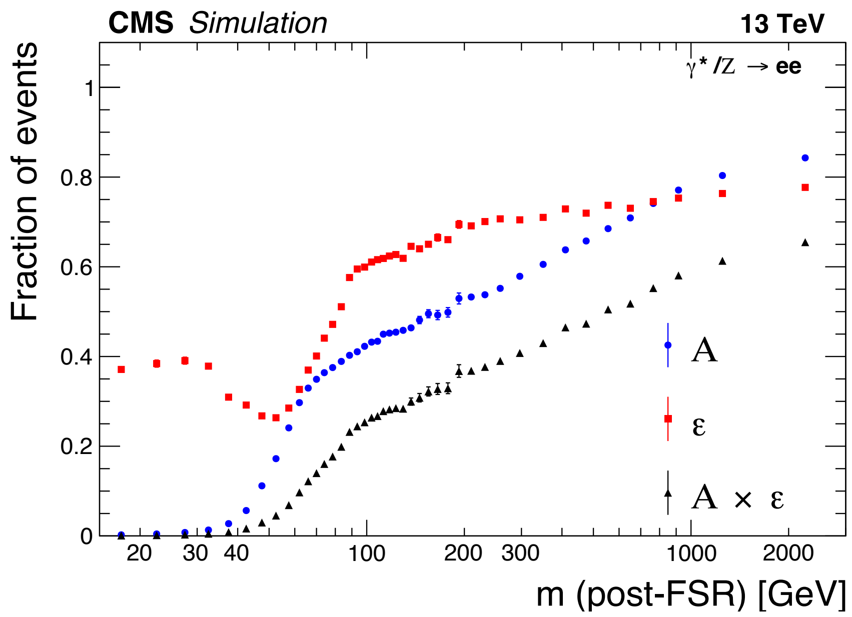
CMS Simulation
13 TeV
$\gamma^*/Z \to ee$
Fraction of events
A
ε
A × ε
m (post-FSR) [GeV]

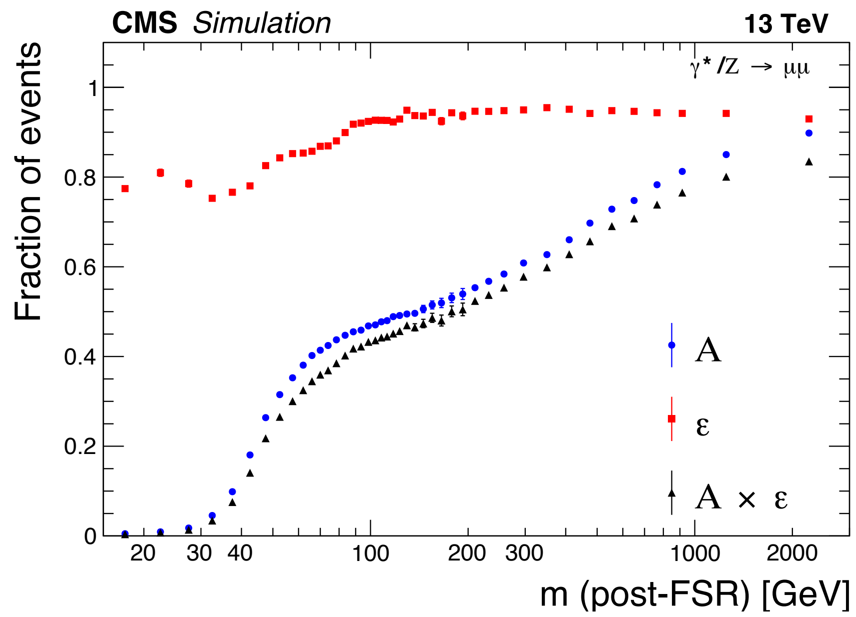
CMS Simulation
13 TeV
$\gamma^*/Z \to \mu\mu$
Fraction of events
A
ε
A × ε
m (post-FSR) [GeV]

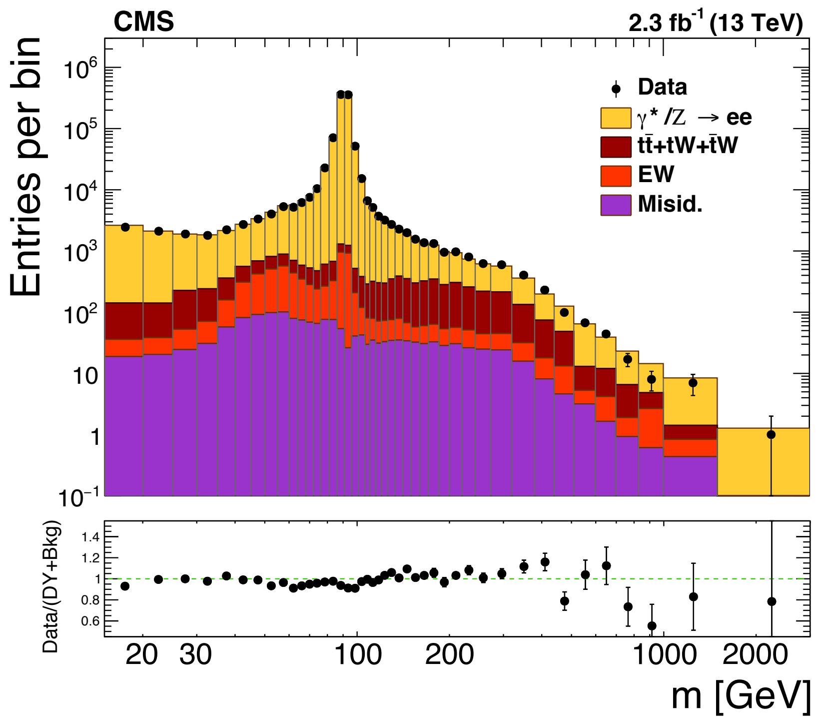
CMS
2.3 fb^{-1} (13 TeV)
Entries per bin
Data
$\gamma^*/Z \to ee$
$t\bar{t}$+tW+$\bar{t}$W
EW
Misid.
Data/(DY+Bkg)
m [GeV]

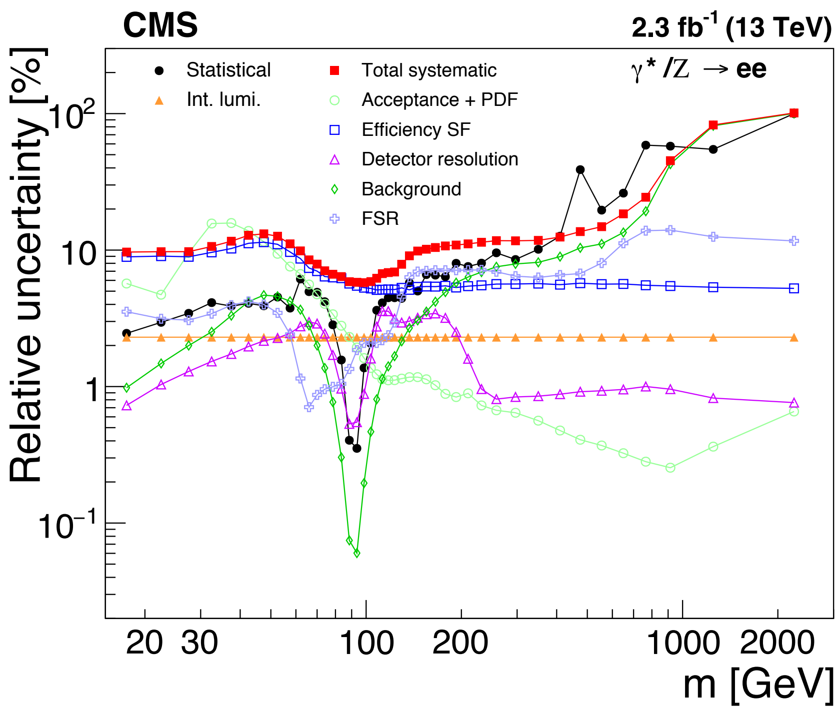
CMS
2.3 fb^{-1} (13 TeV)
$\gamma^*/Z \to ee$
Statistical
Int. lumi.
Total systematic
Acceptance + PDF
Efficiency SF
Detector resolution
Background
FSR
Relative uncertainty [%]
m [GeV]

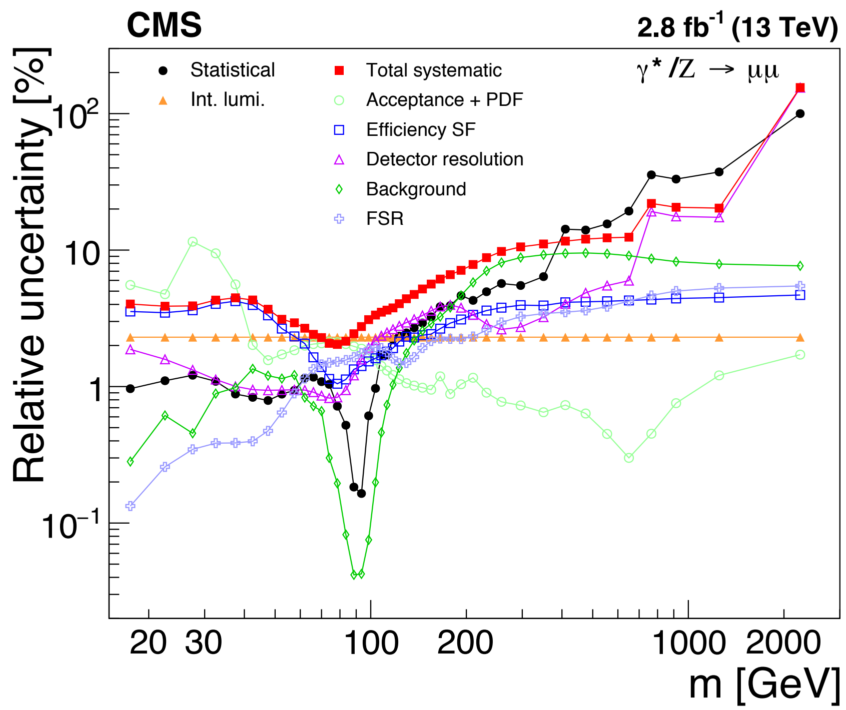
CMS
2.8 fb^{-1} (13 TeV)
$\gamma^*/Z \to \mu\mu$
Statistical
Int. lumi.
Total systematic
Acceptance + PDF
Efficiency SF
Detector resolution
Background
FSR
Relative uncertainty [%]
m [GeV]

Z at 13TeV

Full phase space with dressed leptons

dressed: four-momenta of all simulated photons originating from the leptons are summed within a cone of $\Delta R < 0.1$ around the candidate lepton

Fiducial cross section with leptons after FSR

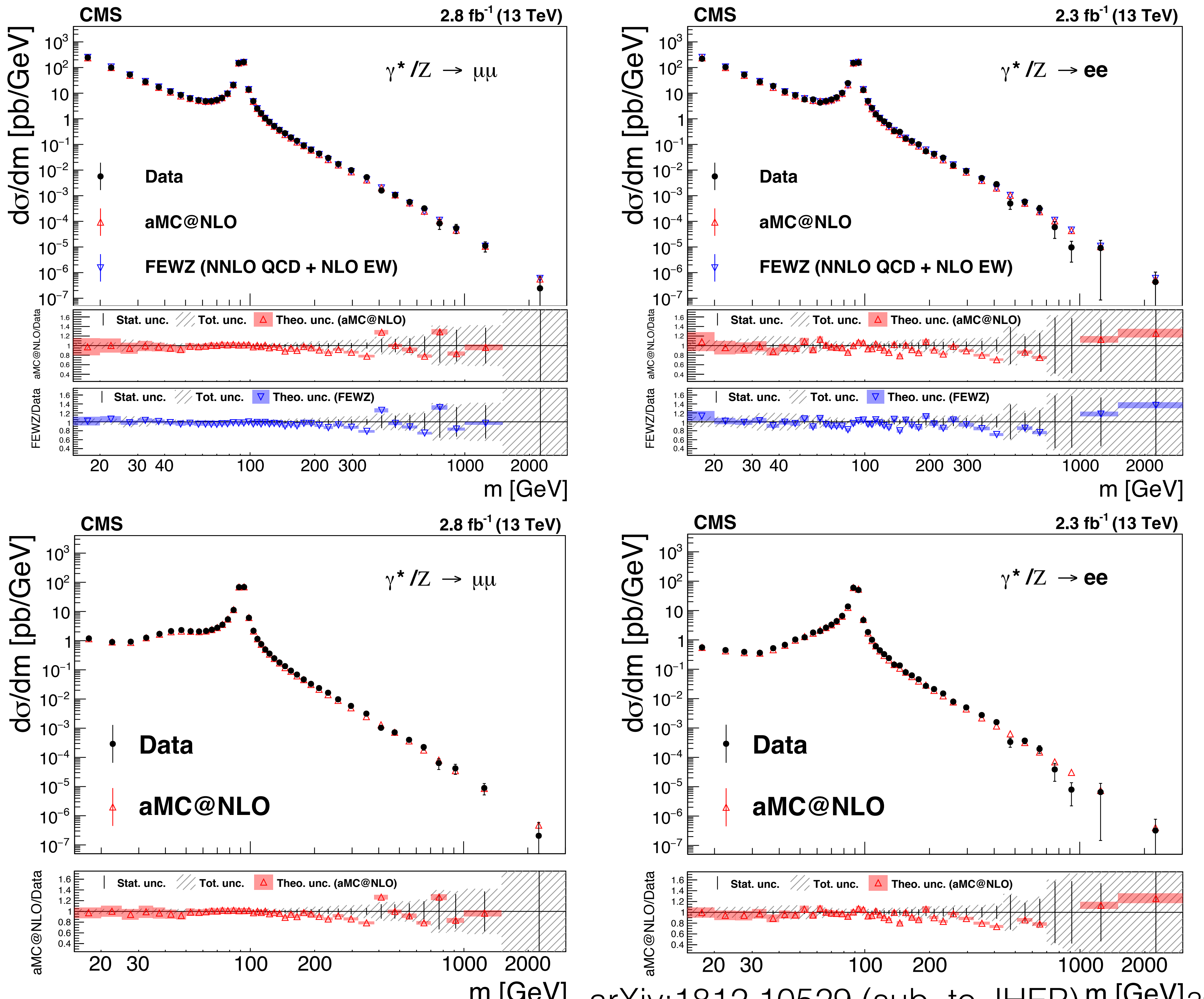

D. Zanzi

arXiv:1812.10529 (sub. to JHEP)

Z at 13 TeV

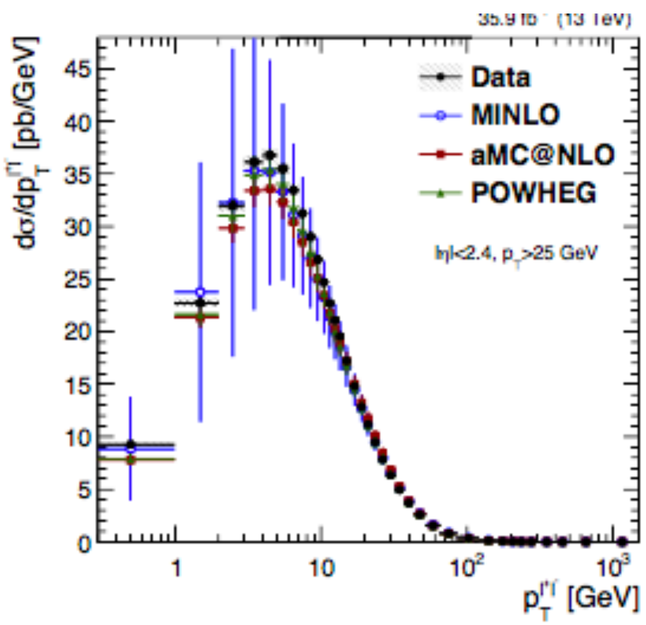

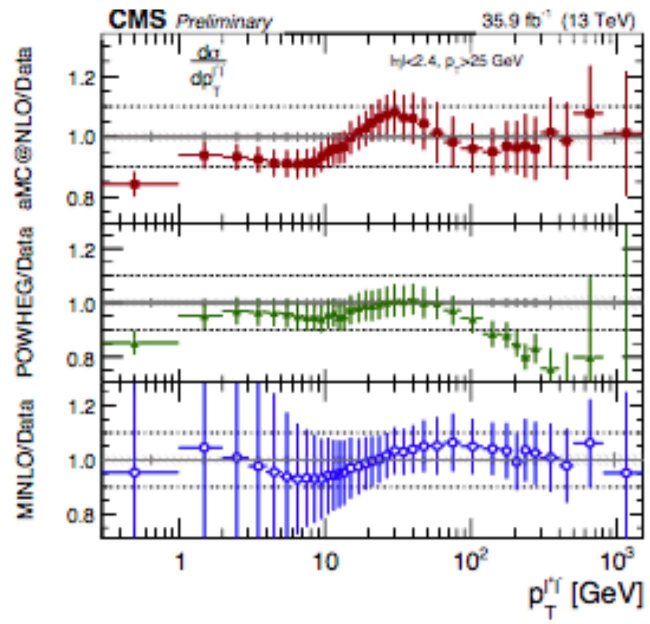

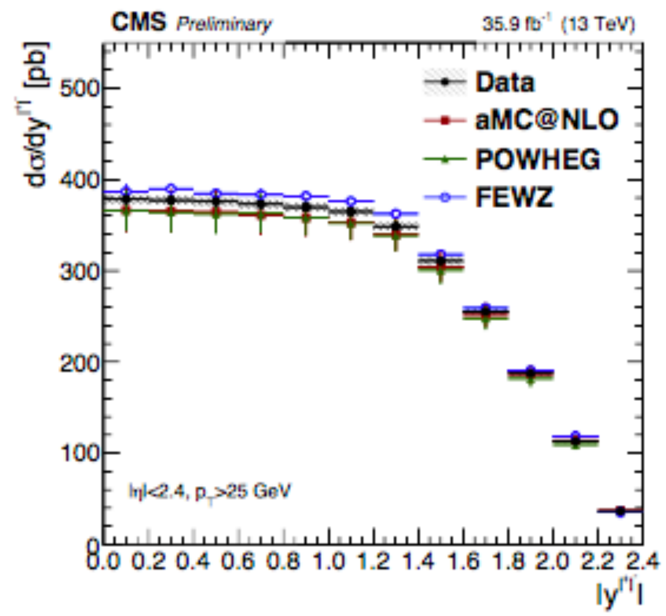

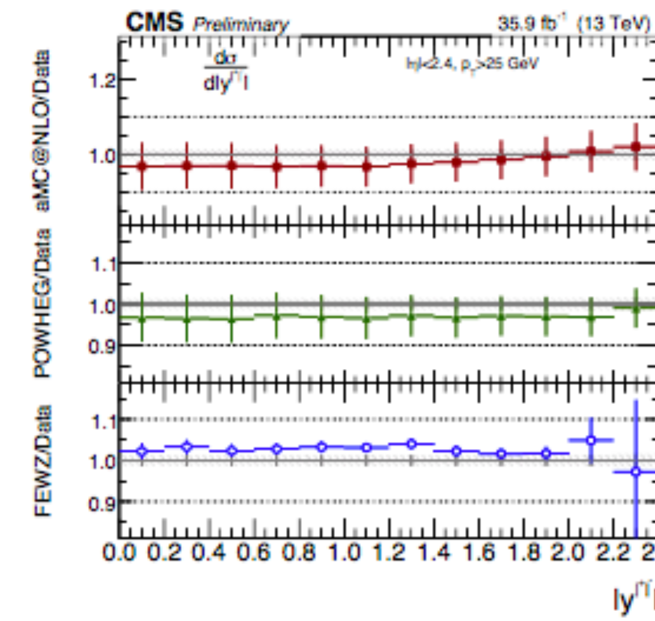

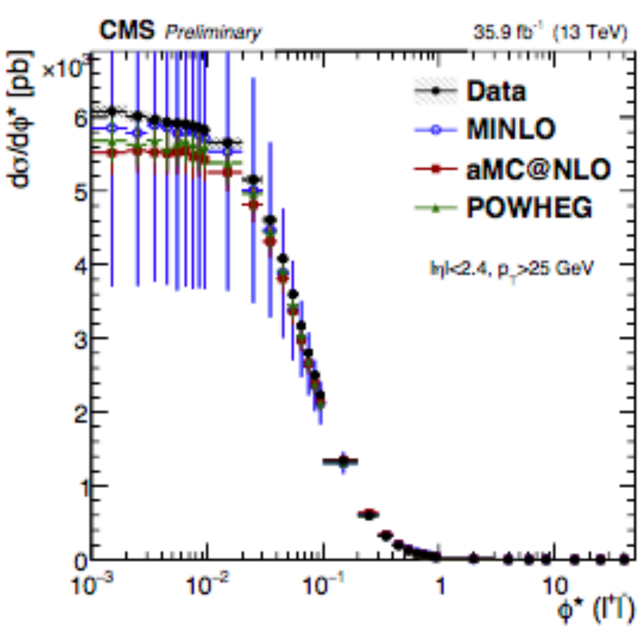

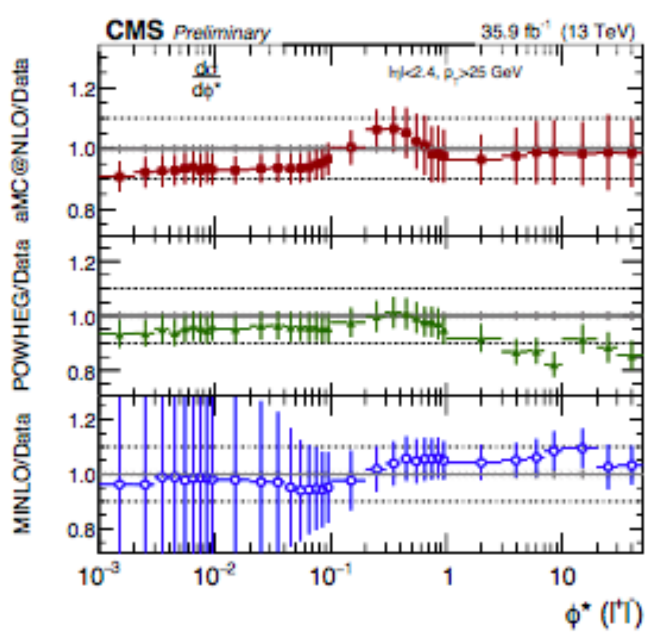

- absolute cross sections

$$\phi^* = \tan\left(\frac{\pi - \Delta\phi}{2}\right)\sin(\theta^*_\eta)$$

$$\cos(\theta^*_\eta) = \tanh\left(\frac{\eta^- - \eta^+}{2}\right),$$

$$\phi^* \sim p_T^Z / m_{\ell\ell}$$

Z at 13 TeV

Absolute cross sections | Normalised cross sections

p_T^{ll}

y^{ll}

ϕ^*

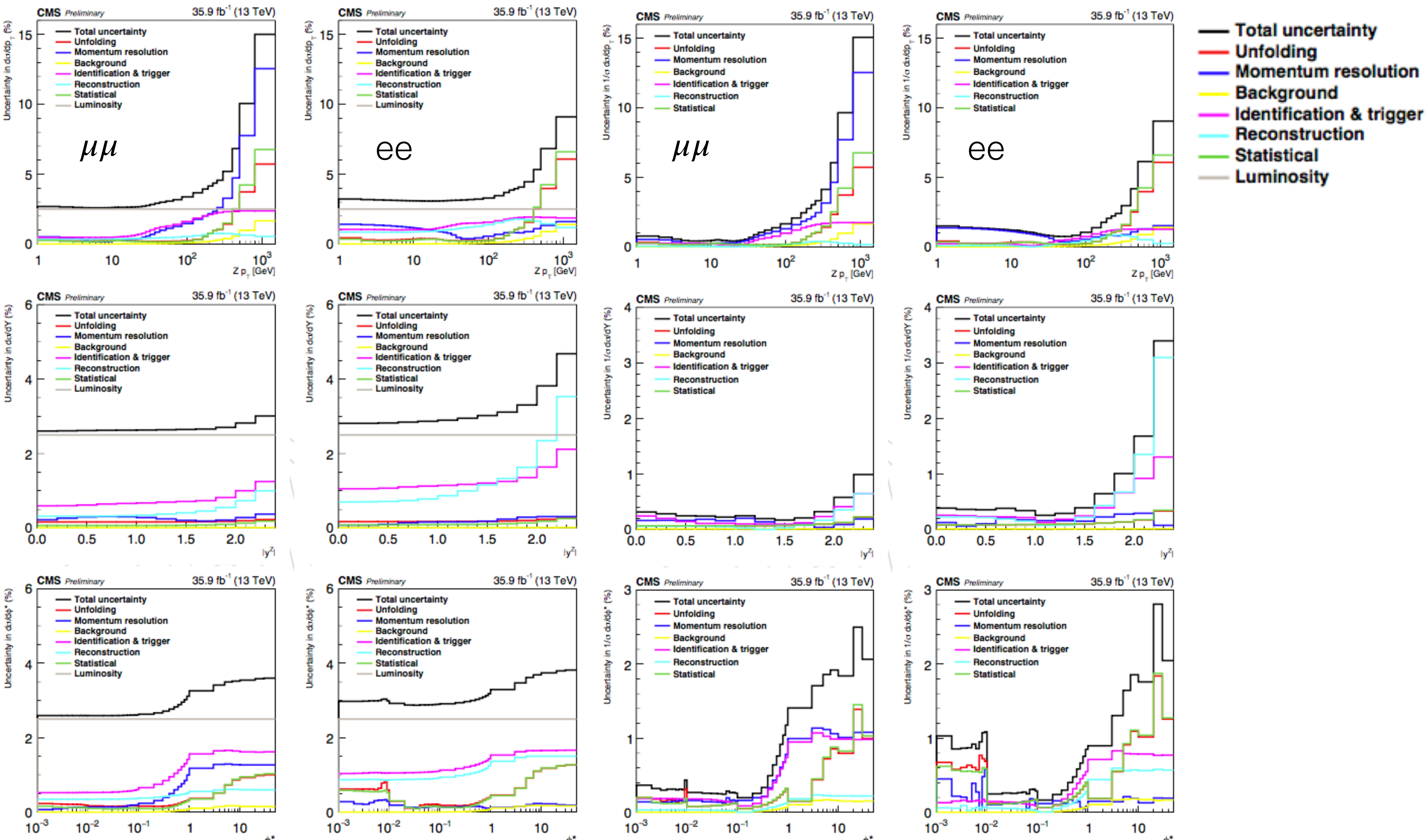

$W \to \mu\nu$ at 8TeV

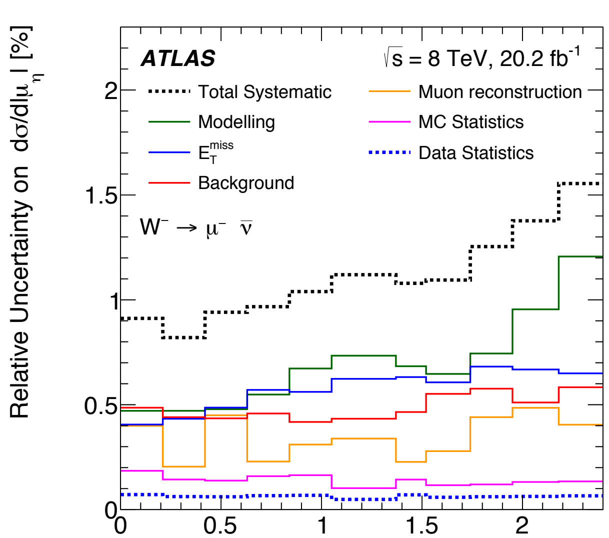

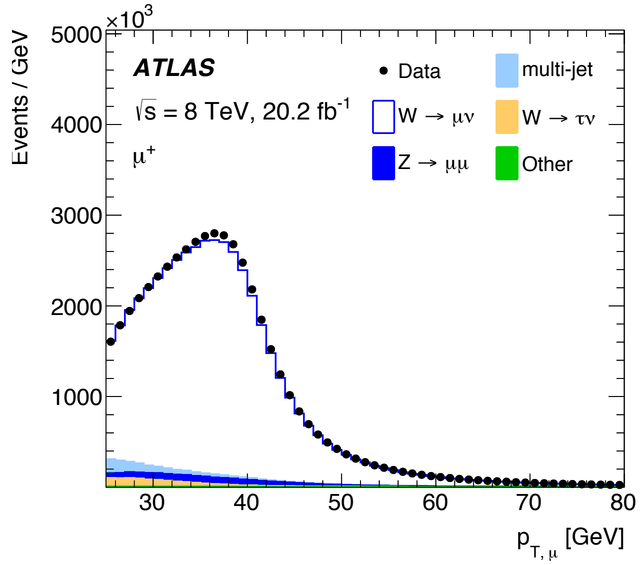

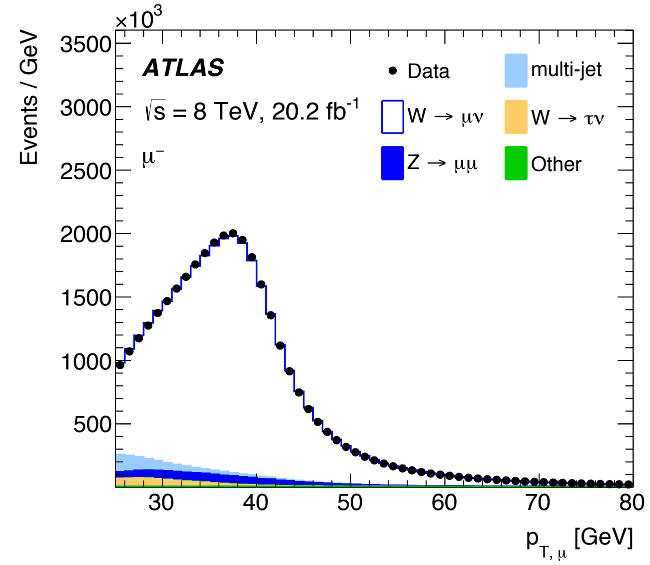

	$W^+ \to \mu^+\nu$	$W^- \to \mu^-\bar{\nu}$
	Number of events	
Data	50 390 184	34 877 365
	Percentage of data	
Multijet	2.4 ± 0.3	3.1 ± 0.3
$W \to \tau\nu$	1.9 ± 0.1	2.0 ± 0.1
$Z \to \mu\mu$	3.1 ± 0.2	4.0 ± 0.2
Others	0.62 ± 0.02	0.82 ± 0.03

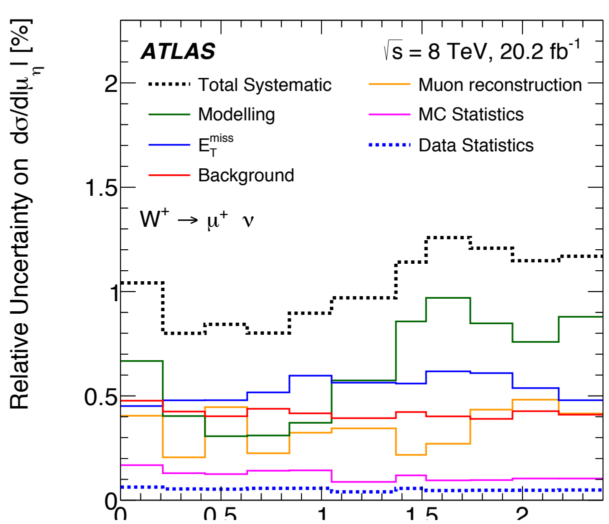

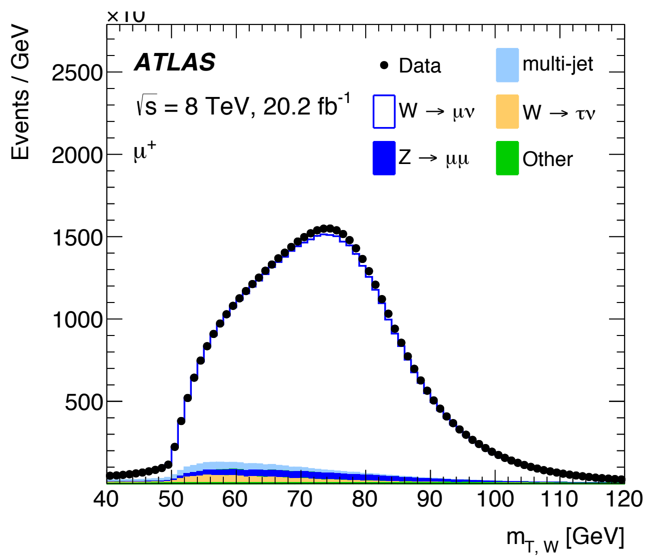

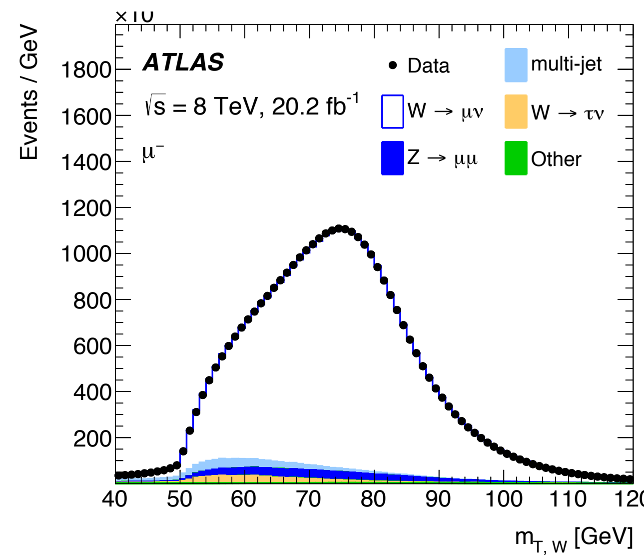

$\|\eta_\mu\|$	$W^+ \to \mu^+\nu$	$W^+ \to \mu^+\nu$
0.00–0.21	0.508 ± 0.004	0.505 ± 0.004
0.21–0.42	0.684 ± 0.004	0.679 ± 0.004
0.42–0.63	0.702 ± 0.005	0.702 ± 0.005
0.63–0.84	0.611 ± 0.004	0.613 ± 0.005
0.84–1.05	0.603 ± 0.004	0.601 ± 0.005
1.05–1.37	0.795 ± 0.006	0.796 ± 0.007
1.37–1.52	0.848 ± 0.008	0.845 ± 0.007
1.52–1.74	0.861 ± 0.009	0.856 ± 0.007
1.74–1.95	0.856 ± 0.009	0.855 ± 0.008
1.95–2.18	0.792 ± 0.008	0.794 ± 0.009
2.18–2.40	0.802 ± 0.008	0.812 ± 0.011
Integrated	0.736 ± 0.003	0.727 ± 0.003

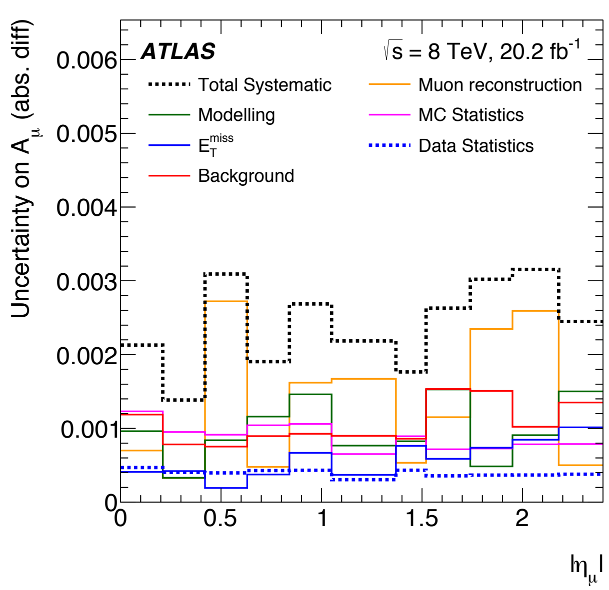

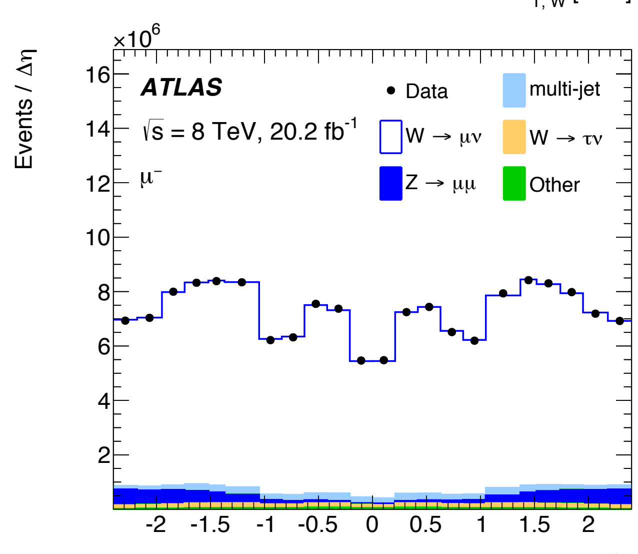

$$m_T = \sqrt{2 p_T^\mu p_T^\nu \left(1 - \cos\left(\phi^\mu - \phi^\nu\right)\right)}$$

$$A_\mu = \frac{d\sigma_{W_{\mu^+}}/d\eta_\mu - d\sigma_{W_{\mu^-}}/d\eta_\mu}{d\sigma_{W_{\mu^+}}/d\eta_\mu + d\sigma_{W_{\mu^-}}/d\eta_\mu}$$

	Data
$\sigma(W^+ \to \mu^+\nu)$ [pb]	3110 ± 0.5 (stat.) ± 29 (syst.) ± 59 (lumi.)
$\sigma(W^- \to \mu^-\bar{\nu})$ [pb]	2137 ± 0.4 (stat.) ± 22 (syst.) ± 41 (lumi.)
Sum [pb]	5247 ± 0.6 (stat.) ± 50 (syst.) ± 100 (lumi.)
Ratio	1.4558 ± 0.0004 (stat.) ± 0.0040 (syst.)
	DYNNLO (CT14 NNLO PDF set)
$\sigma(W^+ \to \mu^+\nu)$ [pb]	3015 ± 92 (PDF) ± 15 (scale)
$\sigma(W^- \to \mu^-\bar{\nu})$ [pb]	2105 ± 53 (PDF) ± 10 (scale)
Sum [pb]	5120 ± 140 (PDF) ± 23 (scale)
Ratio	1.4320 ± 0.0100 (PDF) ± 0.0007 (scale)

[

arXiv:1904.05631 (sub. to EPJC)

$W \rightarrow \mu\nu$ at 8TeV

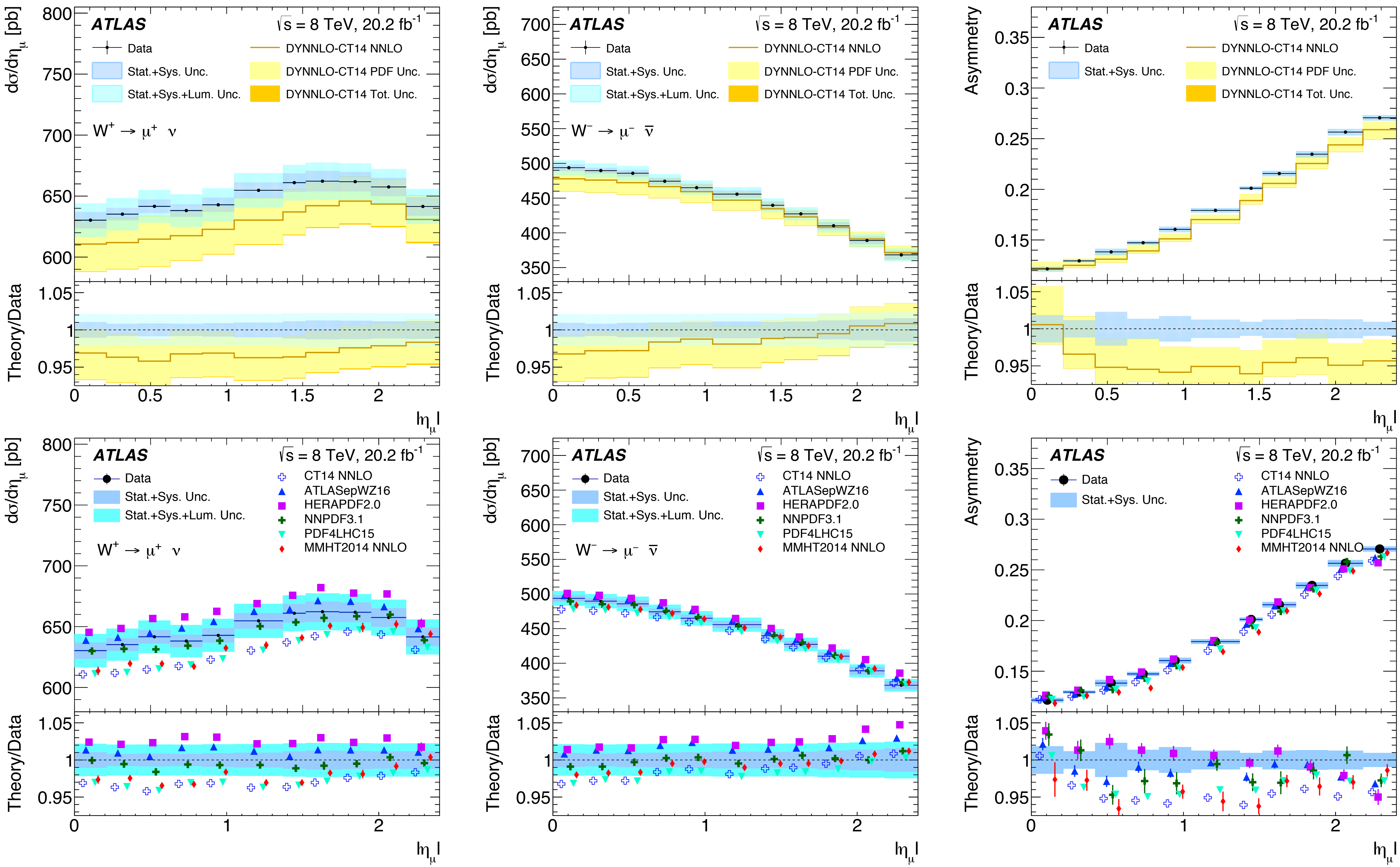

W,Z at 5.02TeV

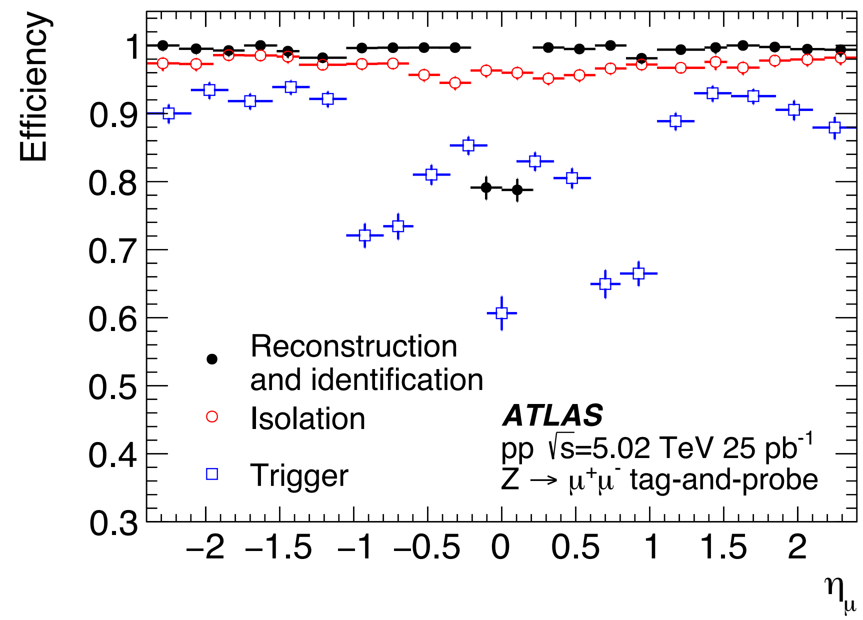

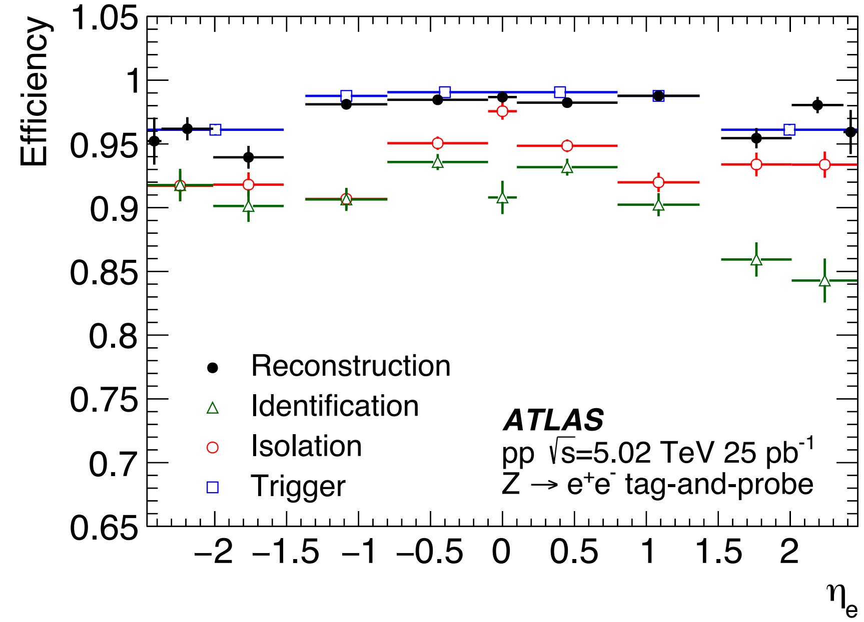

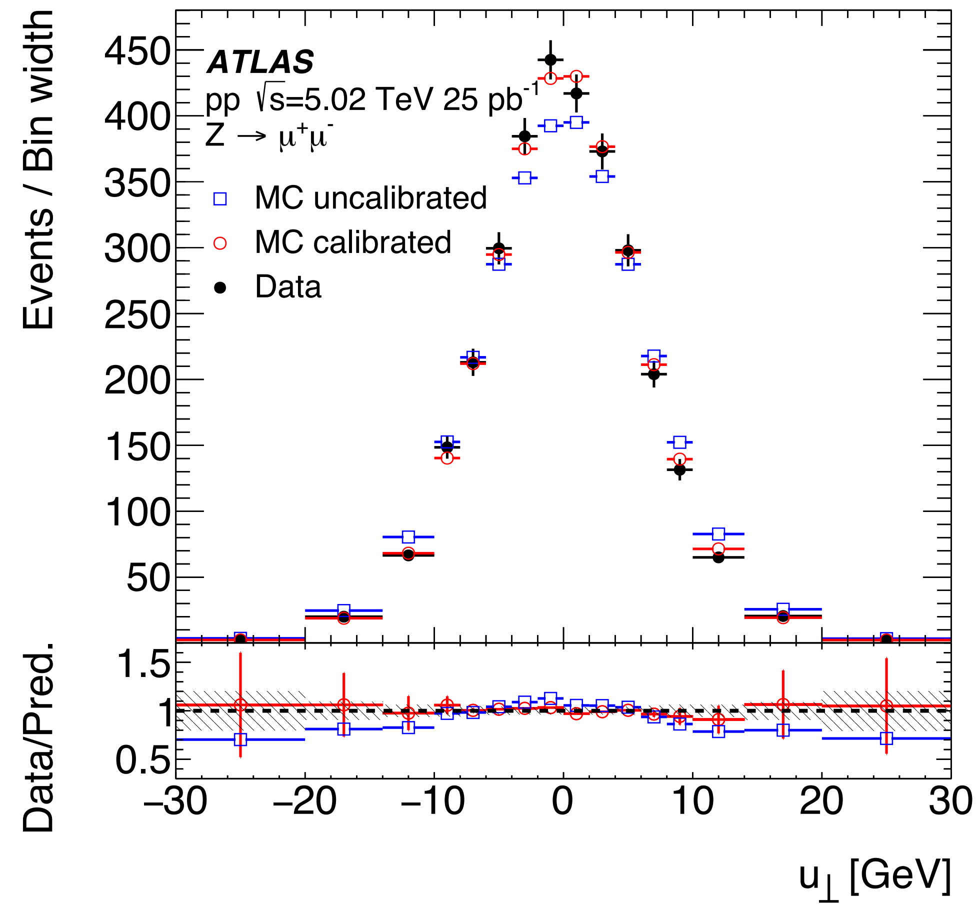

- Precision in lepton efficiency limited by number of Z->ll candidates
- Hadronic recoil with particle flow objects
- Calibration of hadronic recoil based on Z->ll candidates

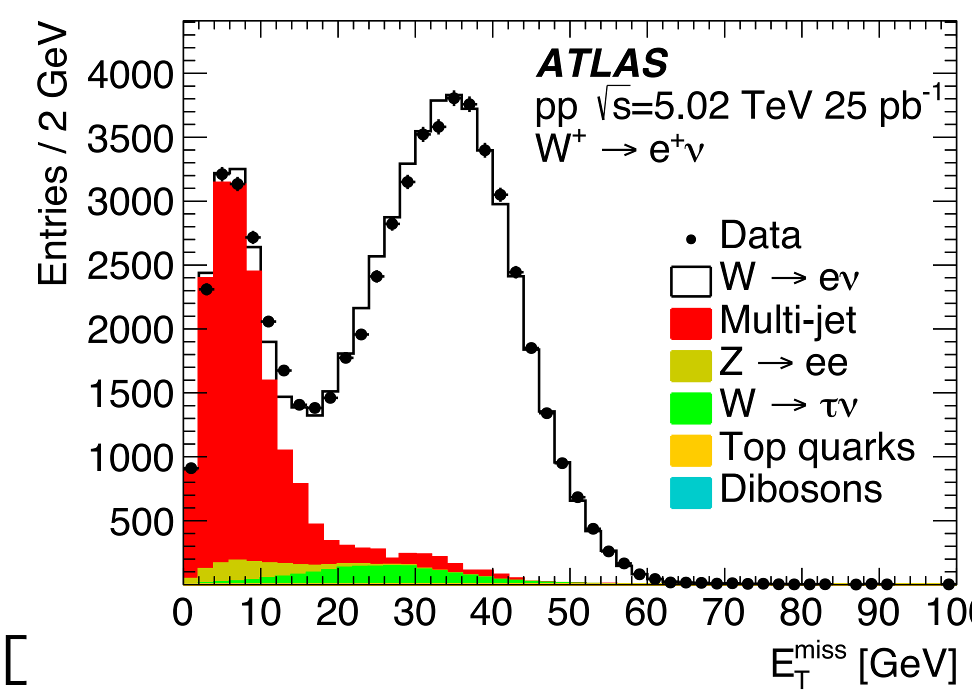

Background	$W^+ \to e^+\nu$ ($W^+ \to \mu^+\nu$) [%]	$W^- \to e^-\nu$ ($W^- \to \mu^-\nu$) [%]	$Z \to e^+e^-$ ($Z \to \mu^+\mu^-$) [%]
$Z \to \ell^+\ell^-$, $\ell = e, \mu$	0.1 (2.8)	0.2 (3.8)	–
$W^\pm \to \ell^\pm\nu$, $\ell = e, \mu$	–	–	<0.01 (<0.01)
$W^\pm \to \tau^\pm\nu$	1.8 (1.8)	1.8 (1.8)	<0.01 (<0.01)
$Z \to \tau^+\tau^-$	0.1 (0.1)	0.1 (0.1)	0.07 (0.07)
Multi-jet	0.9 (0.1)	1.4 (0.2)	<0.01 (<0.01)
Top quark	0.1–0.2 (0.1–0.2)	0.1–0.2 (0.1–0.2)	0.06 (0.08)
Diboson	0.1 (0.1)	0.1 (0.1)	0.14 (0.08)

[

Eur. Phys. J. C 79 (2019) 128

W,Z at 5.02TeV

$$\sigma^{\text{fid}}_{W^\pm\to\ell^\pm\nu[Z\to\ell^+\ell^-]} = \frac{N_{W[Z]} - B_{W[Z]}}{C_{W[Z]} \cdot L_{\text{int}}}$$

$\|\eta_\ell\|^{\text{min}}$	$\|\eta_\ell\|^{\text{max}}$	$W^- \to \ell^-\nu$ dσ/d$\|\eta_\ell\|$ [pb]	$\delta\sigma_{\text{stat}}$ [pb]	$\delta\sigma_{\text{syst}}$ [pb]	$\delta\sigma_{\text{lumi}}$ [pb]
0.00	0.21	329	5	8	6
0.21	0.42	315	5	6	6
0.42	0.63	315	5	6	6
0.63	0.84	298	5	6	6
0.84	1.05	303	5	7	6
1.05	1.37	286	4	5	6
1.37	1.52	276	7	7	5
1.52	1.74	272	4	6	5
1.74	1.95	249	4	5	5
1.95	2.18	253	4	6	5
2.18	2.50	219	4	6	4
0.00	2.50	1401	7	18	27

$\|\eta_\ell\|^{\text{min}}$	$\|\eta_\ell\|^{\text{max}}$	$W^+ \to \ell^+\nu$ dσ/d$\|\eta_\ell\|$ [pb]	$\delta\sigma_{\text{stat}}$ [pb]	$\delta\sigma_{\text{syst}}$ [pb]	$\delta\sigma_{\text{lumi}}$ [pb]
0.00	0.21	456	6	11	9
0.21	0.42	467	6	9	9
0.42	0.63	471	6	9	9
0.63	0.84	460	6	10	9
0.84	1.05	471	6	11	9
1.05	1.37	474	5	9	9
1.37	1.52	482	9	15	9
1.52	1.74	474	6	11	9
1.74	1.95	465	6	11	9
1.95	2.18	446	6	10	9
2.18	2.50	371	5	10	7
0.00	2.50	2266	9	29	43

$\|y_{\ell\ell}\|^{\text{min}}$	$\|y_{\ell\ell}\|^{\text{max}}$	$Z \to \ell^+\ell^-$ dσ/d$\|y_{\ell\ell}\|$ [pb]	$\delta\sigma_{\text{stat}}$ [pb]	$\delta\sigma_{\text{syst}}$ [pb]	$\delta\sigma_{\text{lumi}}$ [pb]
0.0	0.5	103.0	1.7	1.2	1.9
0.5	1.0	101.3	1.8	1.1	1.9
1.0	1.5	89.6	1.7	0.9	1.7
1.5	2.0	60.5	1.4	0.7	1.1
2.0	2.5	20.0	0.9	0.4	0.4
0.0	2.5	374.5	3.4	3.6	7.0

$R^{\text{fid}}_{W^+/W^-}$	1.617 ± 0.012 (stat) $\pm$ 0.003 (syst)
$R^{\text{fid}}_{W/Z}$	9.81 ± 0.13 (stat) $\pm$ 0.01 (syst)
$R^{\text{fid}}_{W^+/Z}$	6.06 ± 0.08 (stat) $\pm$ 0.01 (syst)
$R^{\text{fid}}_{W^-/Z}$	3.75 ± 0.05 (stat) $\pm$ 0.01 (syst)

$\|\eta_\ell\|^{\text{min}}$	$\|\eta_\ell\|^{\text{max}}$	A_ℓ	δA_{stat}	δA_{syst}
0.00	0.21	0.163	0.010	0.001
0.21	0.42	0.195	0.009	0.001
0.42	0.63	0.201	0.009	0.001
0.63	0.84	0.213	0.010	0.001
0.84	1.05	0.218	0.010	0.001
1.05	1.37	0.248	0.008	0.001
1.37	1.52	0.272	0.014	0.002
1.52	1.74	0.271	0.009	0.001
1.74	1.95	0.300	0.010	0.001
1.95	2.18	0.276	0.010	0.001
2.18	2.50	0.256	0.010	0.001

Eur. Phys. J. C 79 (2019) 128

Z3D

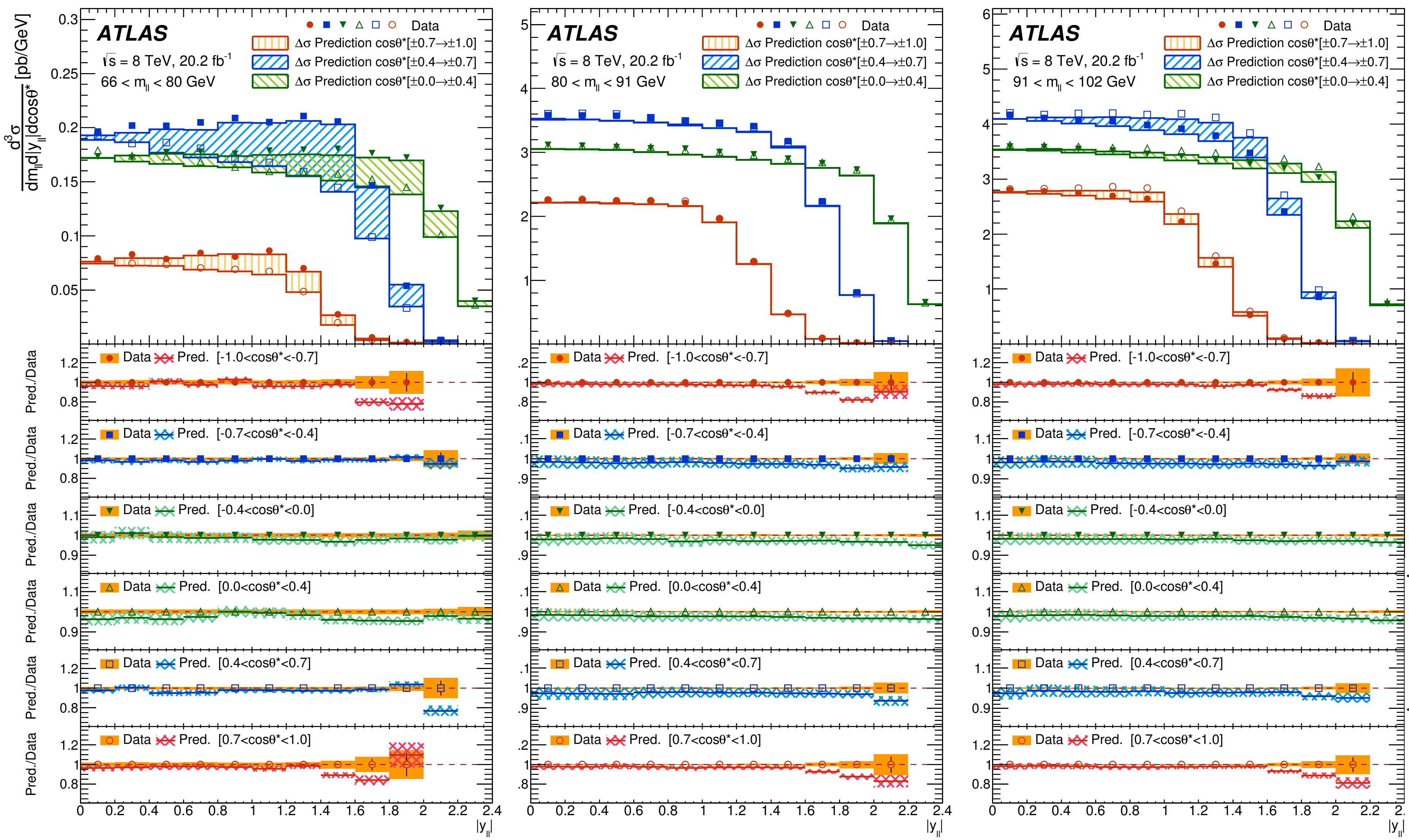
ATLAS
√s = 8 TeV, 20.2 fb-1
66 < mll < 80 GeV
80 < mll < 91 GeV
91 < mll < 102 GeV
Data
Δσ Prediction cosθ*[±0.7→±1.0]
Δσ Prediction cosθ*[±0.4→±0.7]
Δσ Prediction cosθ*[±0.0→±0.4]
d3σ/dmll d|yll| dcosθ* [pb/GeV]
Pred./Data
Data Pred. [-1.0<cosθ*<-0.7]
Data Pred. [-0.7<cosθ*<-0.4]
Data Pred. [-0.4<cosθ*<0.0]
Data Pred. [0.0<cosθ*<0.4]
Data Pred. [0.4<cosθ*<0.7]
Data Pred. [0.7<cosθ*<1.0]
|yll|

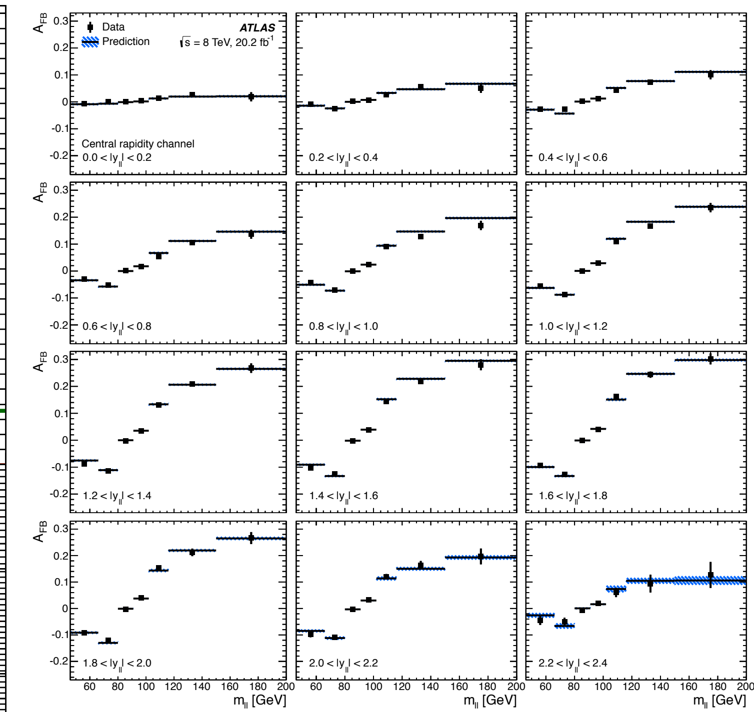
Data
Prediction
ATLAS
√s = 8 TeV, 20.2 fb-1
Central rapidity channel
AFB
mll [GeV]

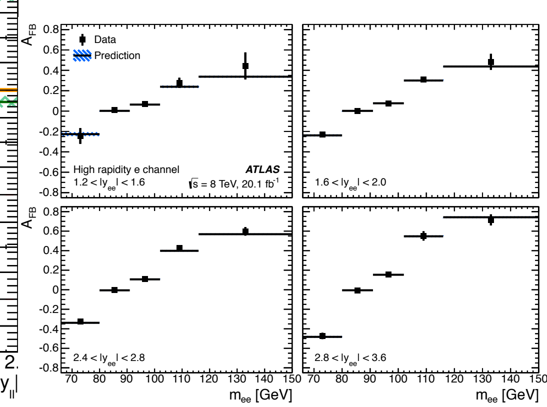
Data
Prediction
High rapidity e channel
ATLAS
√s = 8 TeV, 20.1 fb-1
AFB
mee [GeV]